Chancellor's Honors Program Projects

Supervised Undergraduate Student Research and Creative Work

4-2009

Mobile Electron Beam for Food Irradiation

John Andrew Ritchie
University of Tennessee - Knoxville

Follow this and additional works at: https://trace.tennessee.edu/utk_chanhonoproj

Mobile Electron Beam for Food Irradiation

Group Members:

Rob Burgin
James Bevins
Trey Kauerz
Adam Tuesburg
John Ritchie
Ben Malkey

April 22, 2009

Faculty Advisor
Dr. M.L. Grossbeck

Nuclear Engineering Department
The University of Tennessee

Acknowledgments

Abstract

Food spoilage is a problem that affects people worldwide. Whether it results in increased prices of food in the developed world, or, more direly, in the deaths of people due to starvation in developing countries, it is a problem well worthy of pursuing means of alleviation.

The purpose of this project was to design a mobile food irradiation device to mediate the effects of food spoilage. Three primary means of irradiation were investigated: Cobalt 60 (a radionuclide source), X-rays, and an electron beam source. The e-beam source was selected, due to the limiting weight of the necessary shielding for the other two sources.

Strawberries were selected as the food product to be irradiated. An electron beam source was chosen that would provide the appropriate dose. Shielding and food dose calculations were performed, and a device was designed with appropriate shielding, safety features, and an efficient means of moving the food through the device. A means of transporting the device was developed and a reasonable method for processing the food was established.

The mobile food irradiator is capable of processing over 500 kg of strawberries per hour. The capital cost of one device is approximately $1,350,000.

3

Table of Contents

List of Figures

List of Tables

1.0 Introduction

Ionizing radiation can be used to kill microorganisms in food, which are responsible for spoilage and food born diseases. To this end, the effects of food irradiation are similar to pasteurization in that the objective is to slow the biological processes that cause foods to spoil and therefore extend its shelf life.

The process of irradiating foods for consumption occurs in at least forty nations. The amount of food irradiated per year worldwide is approximately 500,000 metric tons, which is only 0.01% of all food produced[1]. A real-world practical use of food irradiation is to allow the exportation of foods that would otherwise spoil en route to foreign markets. Some Hawaiian Papaya for example, is irradiated prior to being shipped to the contiguous United States[2].

The safety concerns regarding the irradiation of food are considerable. The doses required to sterilize food range from orders of 1 to 10 kGy[1], which would be certainly fatal to a human. To this end, extreme caution must be practiced in the design and operation of such facilities to prevent the unnecessary exposure of radiation to people working at these facilities. Safety features including shielding, interlocks, and procedures are used to provide a reasonable level of safety while working around such powerful sources of radiation.

Cobalt-60, a popular isotope used for food irradiation, constantly emits gamma radiation and cannot be switched off. Additionally, its 5.3 year half life means that it must be frequently replenished. It is, however, an effective and penetrating source of radiation that requires no electricity to operate. Other popular irradiation applications for Cobalt-60 include medical supply sterilization and treatment.

Electron Beam (E-Beam) accelerators send electrons into food at near the speed of light, which creates radiolytic products which prevents cell from continuing to live or multiply. E-Beam machines can also be used to indirectly produce x-ray radiation, which is how x-ray machines work. Electrons themselves by nature are not as penetrating as gamma rays or x-rays, so e-beam machines are limited to irradiating thin targets. An issue particular to the use of accelerator systems is not the shielding concerns of accelerated electrons, but rather the bremsstrahlung radiation produced as electrons slow down in a medium. The photons emitted by this phenomenon are extremely penetrative and constitute the greatest shielding concern in this project.

Figure 1.1: An E-Beam food irradiation facility

Food irradiation is regulated by the Food and Drug Administration (FDA) along with other agencies. The FDA generally considers the process safe, and determines the minimum and maximum dose requirements for irradiated foods. Irradiated foods have not been found to be toxic, radioactive, or otherwise dangerous. Some foods, such as milk cannot be irradiated without significant changes to taste, however[3].

Figure 1.2: The international symbol for irradiated food, called "Radura[4]"

Traditional irradiation facilities cost one to five million dollars to construct, plus operation and maintenance costs. The cost per unit weight to irradiate food varies from one to twenty cents per pound, depending on the dose required to effectively treat the food.

2.0 Purpose

2.1 Mobile Irradiator

In October of 2002, the US Department of Agriculture allowed the importation of irradiated produce to the United States. Therefore, irradiators could benefit those countries looking to export fresh fruit and vegetables in the United States. Many large scale irradiation facilities exist across the world, but many foods might experience spoilage during its voyage to a central facility. Therefore it could be advantageous to developing nations for a mobile irradiation facility that could irradiate foods prior to spoilage that would occur while being shipped. While our design will examine the irradiation of strawberries, probably in the United States, the design could translate easily for benefits to developing countries.

Many mobile irradiators existed in the 1970s, and most of them were relatively small designs incorporating Cesium-137 due to smaller shielding requirements. These

designs are mostly obsolete now due to their low capabilities and obsolete technology[6]. Currently, regulations are not in place for mobile irradiators, and the market for existing mobile irradiating solutions is not very well known. The design presented will attempt to build off current technologies to take advantage of the benefits of a mobile food irradiator.

Figure 2.1: A large mobile irradiator (Beijing Institute of Nuclear Engineering)

containing 250,000-curies of cesium-137

While previous mobile irradiators took advantage of radionuclide sources, it seems unlikely that a design of this type would be feasible due to the immense shielding requirements. Radionuclide sources provide a greater amount of penetration, thus leading to the ability to penetrate pallet loads worth of food at a time. Electron accelerators lack this ability and are only able to penetrate a few inches of dense food at a time. But the accelerators benefit in reduced shielding (although still significant) and the ability to safely turn on/off. This safety function could also prove to be more desirable in a regulation setting that would be very cautious with mobile irradiation technologies. Due

to the lack of penetration, a focus would be placed on fruits and fresh produce such as strawberries. These foods would also seem to be ideal for the reduction of spoilage mentioned previously. These were the deciding factors in opting for an accelerator based design. Following the decision of an accelerator based irradiation source, the designs of power supply, shielding, conveyer system, and other components followed. These components will be discussed in following sections in detail.

2.2 Strawberry Irradiation

Irradiation of fresh fruits and vegetables can help extend shelf-life and improve microbial food safety. For models in the design, strawberries were chosen. In 1986, regulations were passed that allow the irradiation of fruits below levels of 1 kGy. It has been shown at these levels the qualities of fresh fruits and vegetables remain mostly unchanged. The appearances remain mostly unchanged. The texture of vegetables remains unchanged while fresh fruits might suffer from a loss in firmness. The changes would appear to be negligible when compared to differences in seasonal, cultivar, and local variations of vegetables. There is also little effect on the taste of fresh produce. Nutritional qualities of the produce are also relatively unchanged. Irradiation does not cause a significant reduction in vitamin C, and the losses that do occur are low when compared to losses that occur during storage. Also at the levels of 1 kGy radiation, 99% of E. Coli can be inactivated. Irradiation of foods has been well perceived by the public, but only after they were informed of the benefits and safety. The uncertainty of how well they would be received in a larger market is still a concern[7].

11

Strawberries along with apples, bananas, mangoes, onions, potatoes, spices, seasonings, meat, poultry, fish, and grains have been irradiated for many years. Strawberries that have been irradiated can stay unspoiled for up to three weeks as opposed to three to five days for untreated strawberries[8]. During the first quarter of 1993, Carrot Top, Inc. in Illinois reported that irradiated strawberries outsold untreated strawberries by a ratio of 20 to 1 to a public that was informed of food irradiation[9].
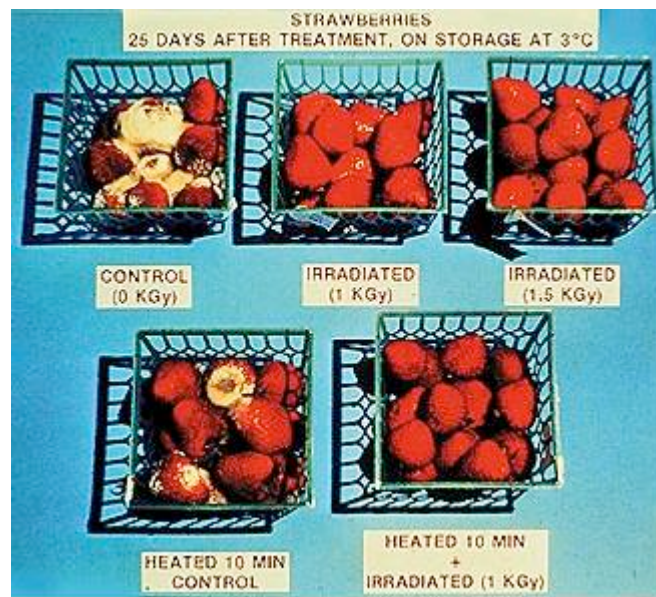
Figure 2.2: Strawberries treated by irradiation

Our design will incorporate the use of strawberries into the dose calculations. Strawberries can possibly be picked in California each month, a few months in Florida and in other states only during a single month.

3.0 Standards and Regulations

3.1 Worker Dose Standards

Recommendations made by the International Commission on Radiological

Protection (ICRP) and by the National Council on Radiation Protection and Measurement

(NCRP) are quite similar, as can be seen in table 3.1.1.

Table 3.1.1 Dose Limits[10]

	NCRP-116	ICRP-60
Occupational Exposure		
Effective Dose Annual	50 mSv	50 mSv
Effective Dose Cumulative	10 mSv X age	100 mSv in 5 years
Equivalent Dose Annual	150 mSv lens of eye 500 mSv skin, hands, feet	150 mSv lens of eye 500 mSv skin, hands, feet
Exposure to Public		
Effective Dose Annual	1 mSv if continuous 5 mSv if infrequent	1 mSv, higher if needed, provided 5-y annual average less than 1 mSv
Equivalent Dose Annual	15 mSv lens of eye 50 mSv skin, hands, feet	15 mSv lens of eye 50 mSv skin, hands, feet

Radiation limits are set with the idea that mankind is reaping some benefit from a

process that involves exposing people to radiation. Different standards apply to members

of the general public versus people exposed to the radiation as part of their jobs. The

reasoning behind the difference is that workers are knowingly exposing themselves to the

radiation and are being compensated to do so. Members of the general public may be

unknowingly exposed or may be part of groups of special concern such as pregnant

women or children, and are hence protected by much more stringent standards[10].

The standards, both occupational and for members of the public, are designed to

compensate for radiation a person may have been exposed to through everyday life such a

for medical x-rays and background radiation.

ALARA is an acronym referring to the spirit in which the control of radiation exposure should be approached: As Low As Reasonably Achievable. The standards set forth by the ICRP and the NCRP should be viewed as maximum limits not to be exceeded, rather than goals to strive for. In this project radiation exposure was minimized even when not required by limits, in accordance with the ALARA principle.

3.2 Food Irradiation Standards

Three terms are used in classifying food radiation doses. Radurization: doses of less than 1 kGy intended for vegetable sprouting, fruit ripening, and insect sterilization. Radicidation: doses of 1 to 10 kGy intended to kill most pathogens, many food organisms, and insects and parasites. Rapperitization: doses greater than 10 kGy that sterilize the food by killing all bacteria and viruses[1]. The objective for this mobile food irradiation device is Radurization. Radurization kills insects and increases shelf life.

The regulation for fruit and vegetable irradiation determined by the FDA in 1986 sets the irradiation limit for fruits and vegetables in the United States at less than 1 kGy. Additionally, the FDA requires that the food receive at least the minimum dose required to achieve the desired goal[11]. An appropriate dosage for radurization of strawberries is from 0.4 to 1.0 kGy[1].

The FDA requires that the food irradiation conform to a scheduled process. This scheduled process means that a written procedure must be in place and strictly followed to carry out the irradiation process. The main purpose of this scheduled process is to ensure that the food receives the appropriate dosage for the given processing conditions.

The FDA requires that records of the irradiation process be kept by the irradiator for three years or for one year after the shelf life of the product has expired, whichever is

shorter. The records should include date of the irradiation, the dose distribution in the product, dosimetry, source calibration, ionizing energy source, scheduled process, evidence of compliance with the scheduled process, lot identification, and the type of food treated[11].

The radiation source used in this design is an electron beam. The limit set on the energy of the electrons of the electron beam as set by the FDA is 10 million electron-volts (MeV)[11].

For pre-packaged foods, the type of packaging that may be put through the irradiation process is dictated by the FDA[11]. For strawberries, many of the existing packaging materials are approved for doses of less than 1KGy.

3.3 Vehicle Regulations

The Federal Highway Administration, a division of the U.S. Department of Transportation, establishes commercial vehicle weight and size standards for vehicles travelling on the nation's Interstate Highway System. While states have the ultimate authority in what the limits will be in each state, the federal government will forfeit all highway funds to any state that does not at least enforce their minimum weight standard, and civil actions can be brought by the Department of Justice against those that violate size standards.   All of the fifty states currently enforce the minimum standards. Exceptions are permissible for indivisible loads that must exceed the standards, and are granted through the states on a case by case basis.

The maximum gross vehicle weight permissible on the interstate highway system is 80,000 pounds[12]. The distribution of the weight is also important. In order to comply with the Bridge Formula established in 1975 (an act to protect our nations system of

Bridges), the following Formula must be used: W=500[LN / N-1 + 12N + 36], where L

is the distance in feet between the outer axles of any group of two or more consecutive

axles, W is the overall gross weight on any group of two or more consecutive axles to the

nearest 500 lbs, and N is the number of axles in the group under consideration[12].

  The federal government establishes no standard of overall vehicle length, with the

exception of vehicles carrying boats or other vehicles. Similarly, no trailer maximum

length is established, but rather the states are required not to limit trailers to less than 48

feet. No state may impose a limitation on width that is either greater or less than 102

inches. Mirrors are not considered in the calculation of width. The federal government

has no standards for vehicle height. Limitations enforced by states range from 13.6 feet to

14.6 feet[12].

4.0 Design Overview
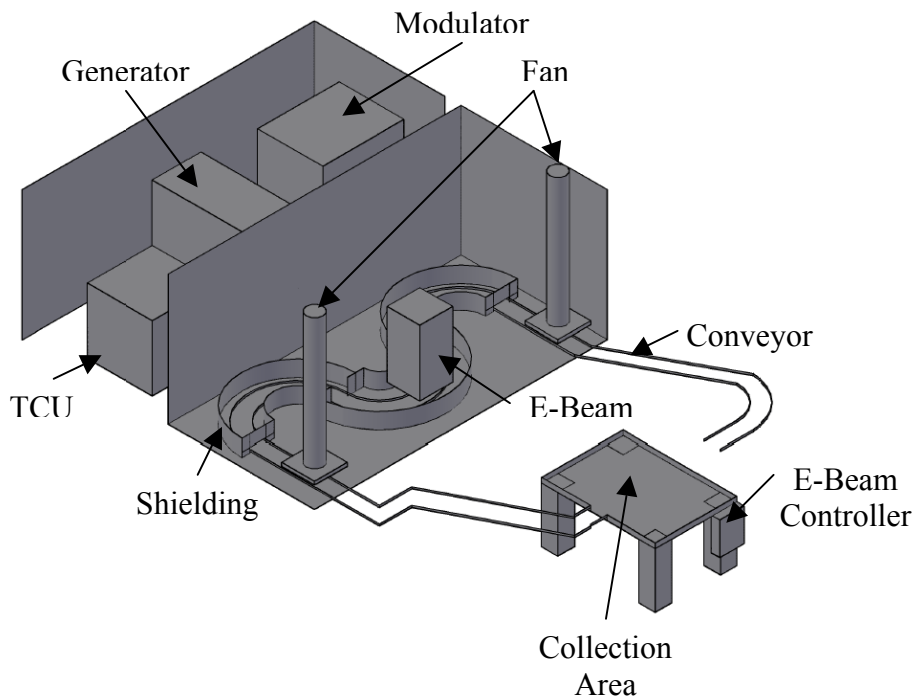
Figure 4.0.1

The above figure 4.0.1 is an AutoCAD drawing of the layout of our mobile

irradiation design. The mobile irradiator is compromised of multiple parts that are

contained in two 20'x 8'x8' Conex boxes. One box contains the Modulator, Generator,

and the TCU (cooler). The other box contains the E-beam, the shielded area, and the

conveyor system that carries the strawberries thru for irradiation. The second figure 4.0.2

below is a side view of the design, showing how the conveyor belt drops down low to the

ground so that when the strawberries are zapped the ground acts a part of the shielding.
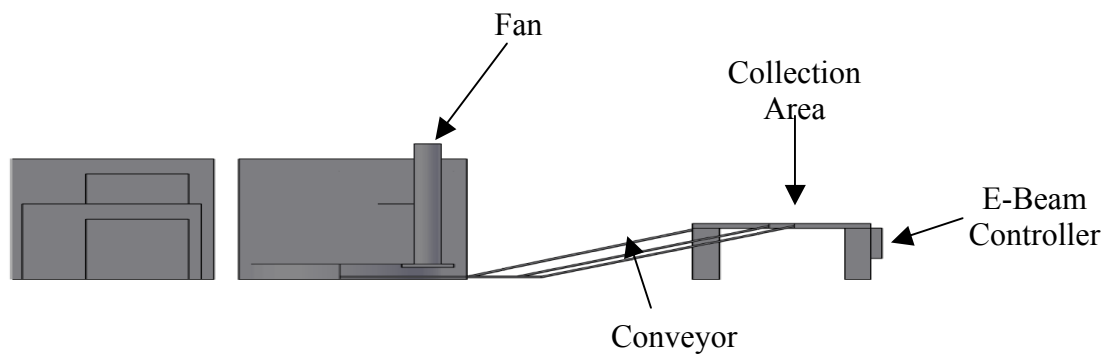
Figure 4.0.2

4.1 Electron Beam Source

The e-beam machine is custom built by an e-beam supplier. Mr. Paul Leek, of

L&W Research, Inc., provided some of the characteristics of a design well suited for this

application, via e-mail correspondence (see Appendix IV). The unit consists of 4

individual components: the beam head, the modulator/power supply, the TCU (cooler),

and the control.

17

The size of the beam head is 60" by 36" by 36". The scan horn, from which the electrons emerge, extends about 24" from one of the 36" square sides. For an 16" wide scan, the bean horn is 4" wide. The head weighs approximately 700 lbs. It is located adjacent to the conveyor/shielding inside the main box.

The modulator/power supply is a rack about 7' tall by 5' wide by 4"deep. It is located in the trailer, which is separate from the main irradiator box. During operation, the trailer will be located next to the irradiator box. The modulator/power supply weighs about 600 lbs.

The TCU is a refrigerated cooler with 4' by 4' by 4' dimensions. It is located in the trailer with appropriate ventilation. The TCU weighs approximately 500 lbs.

The control unit is a 24" by 18" by 5" touch screen computer. It weighs about 50 lbs. It is stored in the trailer during transport, and set up along side the main box when in operation, where the loading/unloading process is taking place.

The electron beam produces 10 MeV pulses about 5 microseconds wide, with a frequency up to 300 pulses per second. The beam power is 1kW. The power requirement for the e-beam is 15kW 3 phase 208 volts.

The total cost of the electron beam source is approximately $825,000.

4.2 Generator

The generator selected for this project is the Detroit Diesel Model 20-JS6DT4. This generator meets the power requirements for this operation and is small enough to be mounted on a trailer for easy transportation. The generator specifications are given in Table 4.2.1.

Table 4.2.1: Generator Specifications

Model	Detroit Diesel 20-JS6DT4
Power Supplied	20kW 3 Phase-208V
Weight	1684 lbs
Dimensions	52in x 70in x 34 in
Cost	$11,299.20
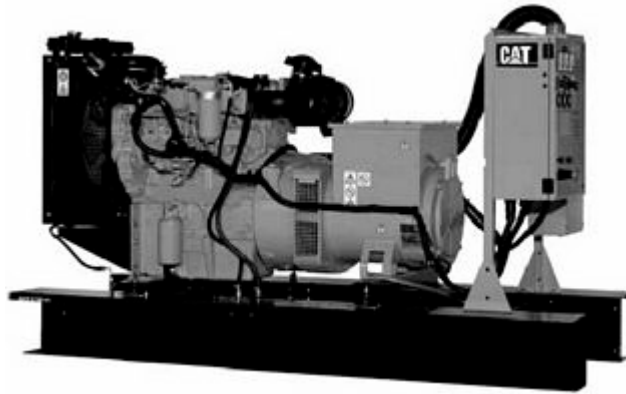
Figure 4.2.1: Diesel generator selected for e-beam operation

4.3 Conveyor

A conveyor system is used to transport the material into, through, and out of the irradiation area. Dorner Conveyor's 7300 series conveyor line is used outside of the irradiation area. The 7300 series meets FDA guidelines for food production applications and is portable. The conveyor frame and most components are stainless steel.

The portion of the conveyor system exposed to the radiation field is custom made by Dorner. The primary material used is ultra-high molecular weight Delrin. The drive mechanism is partially metal (aluminum), but is steel-free. This design minimizes secondary high-energy bremstrahlung radiation production. The belt chosen is also easily replaceable as will be necessary after exposure to the significant doses experienced in the

system. The changing of the belt will be necessary regularly scheduled maintenance whose frequency will depend on quantification of Delrin's capability to withstand high radiation doses.

The conveyor motor control system is flexible as far as power inputs available. It accepts single phase 115V or 230V input voltages, and three phase 230V or 460V input voltages. The system draws approximately 2.5 amps of current.

The cost of the conveyor system is approximately $15,000.

4.4 Truck (PLS)

In order to make the food irradiation facility mobile, a Palletized Loading System (PLS) has been chosen to provide transportation. Manufactured by Oshkosh Defense and pictured in Figure 4.4.1, this truck has the capabilities to transport two International Organization for Standardization (ISO) containers up to 20 feet in length[13,14]. One container is placed on the PLS and the other on a trailer pulled by the PLS, and the containers are loaded and unloaded via a container handling unit. The rugged PLS is built to military standards which ensure its ability to withstand extreme conditions, therefore, making it a reliable choice for this application.

Figure 4.4.1: A PLS loaded with a 20 ft ISO container[15]

The PLS can seat 2 people in its cab. The vehicle has a curb weight of 52,500 pounds with a gross vehicle weight rating of 90,500 pounds. Equipped with a 6-speed automatic Allison Transmission and a 600 hp CAT diesel engine, a PLS is more than capable. A PLS is equipped with ten 20 inch tires located on five axles and one spare. A fully loaded PLS can travel up to 62 mph. The truck is 445 inches long and 96 inches wide and can hold 185 gallons of fuel. The PLS has the ability to steer with its front two axles and its most rear axle. An ISO container is hauled on the PLS and a container handling unit can load and unload the container in under a minute, and unload the PLS and trailer in under 5 minutes, all without stepping out of the vehicle because the controls are located within the cab. With the ability of fording up to 48 inches or climbing a 30 percent grade with up to a 20% side slope, the PLS can reach the most difficult of places in order to provide the necessary food irradiating.

The container handling unit (CHU) pictured in Figure 4.4.2 is a modular add-on installable on a PLS without cutting, drilling, or welding. The CHU is very capable of loading and unloading ISO containers with a misalignment up to a 10% slope, 10% side slope, and 10% offset relative to the truck. The CHU can also load and unload containers that are located 5 feet above ground or even 12 inches below ground.

Figure 4.4.2: A PLS with its CHU extended to unload an ISO container[15]

The cost of a PLS is $360,139 and the cost of the trailer is $46,731 bringing the total for the PLS to $400,970.

4.5 Container

With durability and transportability in mind, a standard ISO container is an obvious choice that matches up well with the abilities of a PLS. A container will be used for the necessary components used for irradiation, and a second container will be used for remaining parts and other materials needed for operation. The standard ISO container has an exterior of corrugated stainless steel. A side view schematic of a PLS loaded with a 20 ft ISO container is shown in Figure 4.5.1. The containers will have dimensions of 20 ft X 8 ft X 8 ft. The model picked for the facility is the All Access Dry Freight ISO Cargo
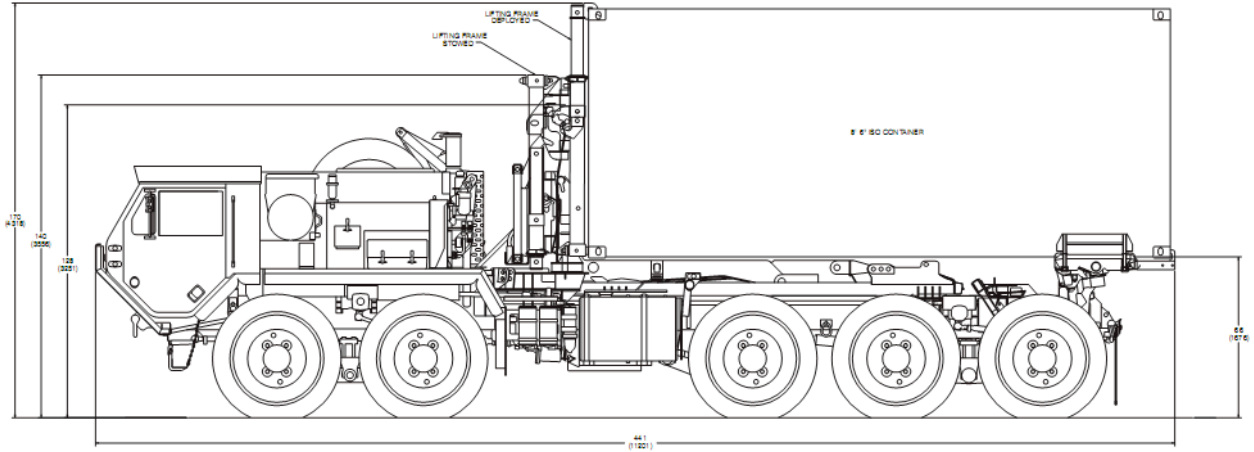
Figure 4.5.1: Side view of a PLS loaded with an ISO container[15]

Container and is manufactured by Sea Box. This ISO container has the ability for a full opening on all 4 sides which means that each side can be used for access and/or maintenance, shown in Figure 4.5.2. The two side doors are made of 14 gauge steel and are double bi-fold swing doors. The two end doors are also composed of 14 gauge steel and are swing doors. The container housing our irradiation facility will be slightly modified. A permanent opening for the conveyor system to enter and exit the container is permanently open. A single container weighs 8,050 pounds. The bases of these containers are tested to hold 16,000 pounds per every 44 square inches, and a max container weight of 44,860 pounds.

Figure 4.5.2: All Access Dry Freight ISO Cargo Container[14]

The approximate cost for two containers is $8,000.

4.6 Shielding: General Design Description

The shielding design for the Minatron must account for the 10MeV electrons generated as well as photons generated through bremsstrahlung, annihilation, characteristic x-rays, and fluorescence. Additionally, the design had the limitations of minimizing weight to comply with Department of Transportation (DOT) regulations while keeping the occupational doses to a minimum.

A major consideration in designing the shield was to provide a low Z shield as the first layer to reduce the amount and energy of the bremsstrahlung radiation generated from the electron interacting with the shield nuclei. As Figure 4.6.1 shows, the flux of the overall energy spectrum can be reduced by lowering the Z of the initial shield. For this reason, a dual layer shield of polyethylene and lead was chosen.

Number of photons of energy k per $m_0 c^2$

Experimental data ▲ Pb
× Sn
✳ Cu
● Al

Photon energy (keV)
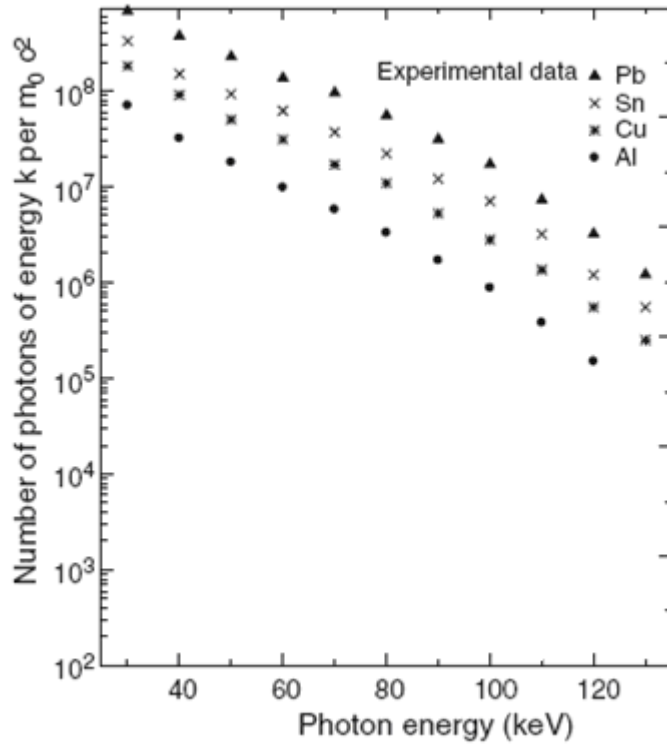
Figure 4.6.1: Dependence of Thick Target Bremsstrahlung Distribution on Z[16]

The polyethylene shield - (C2H4)n - was chosen to be the first layer of defense due to its high hydrogen content and availability. To combat cracking and deformation due to the high radiation flux it will be subjected to, the polyethylene was encapsulated in a thin, 2.5mm aluminum casing. Analysis of this component of the shield is presented in Section 5.0 below.

Lead was chosen as the primary photon shield due to its low cost and high density. The high density allowed for a more compact shield, a key component in making the overall design portable. Steel was used as the structural component of the Conex box instead of lead due to its more favorable structural properties and the desire to minimize exposure to lead which is a toxic substance that can cause lead poisoning among other health issues. For this reason, the primary lead shield was also encapsulated

in a 5mm layer of steel. Analysis of this component of the shield is presented in section 5.0 below. A cross section of the layer shield approach is shown in Figure 4.6.2 below.
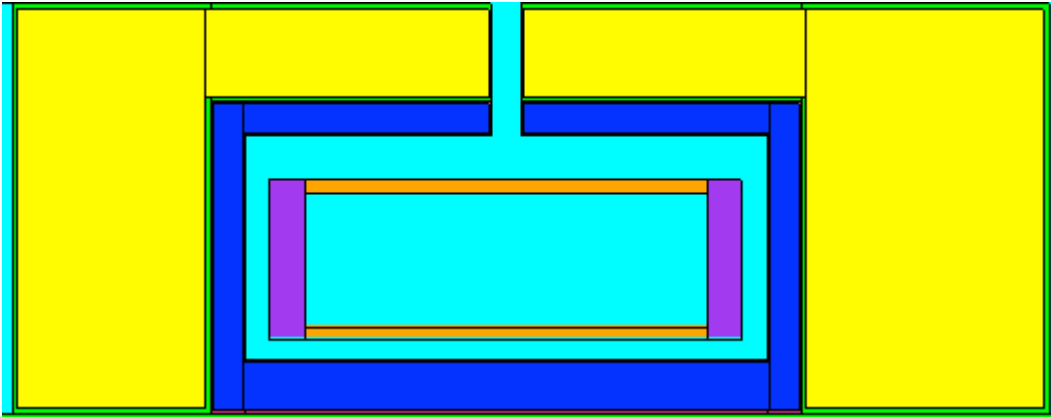
Figure 4.6.2: Cross-sectional view of the layered approach to shielding. Yellow is lead, green is steel, dark blue is poly, red is aluminum, orange and purple are the conveyor, and light blue is air.

Another concern was the entrance of the conveyor into the shielded area. Due to the compact size and weight limitations, there were few options available to ensure that any entrance into the shield did not present a gap where particles could stream unshielded outside the container. This was accomplished with an S-bend in the conveyor that allowed for a small solid angle visible to photons only after multiple scattering, see Section 5.0 below for further analysis.

The final concern, already mentioned above, was the weight of the shield. Due to the intense radiation field, the shield had to be very thick. Therefore, any significant increase in the volume of the shield dramatically increased the gross tonnage of the shield and reduced the practicality of such a design. To minimize shielding weight and meet the other above stated objectives, the shield was placed directly over three sides of the s-

shaped conveyor described above. This minimized the volume of the shield while allowing for greater thickness in high flux areas and lower thickness in lower flux areas as determined by calculations performed by MCNP5. The bottom was left unshielded as the container was placed directly on the ground. For further analysis, see Section 5.0 below.

4.7 Safety

4.7.1 Irradiation Accessibility

The most important safety feature implemented in the design is the lack of accessibility to the irradiation zone. The only access point to the irradiation zone will be the two openings designed for the conveyor system. Since the irradiation beam has such little penetration, the amount of food to be irradiated will be a single clamshell type container. This allows the openings to be small enough to prohibit people from entering the area. This is a passive safety feature that all but eliminates people from accessing the most hazardous and fatal areas of the device.

4.7.2 Conveyor Belt Features

Belt Speed

The belt speed will be monitored using standard techniques. This will allow for proper modeling and control over the amount of dose exposed to the strawberries. The speed of the belt will determine how long the food is under the beam area. If the belt were to stop or slow down, the food might be over exposed thus failing to meet FDA standards. Thus if the belt is not achieving a certain speed, the electron beam will shut down.

Infrared System

In order to ensure that a strawberry container is not lodged or stuck inside the belt path, an infrared system is placed on the outlet of the conveyor belt path. Each time a package passes, the beam is broke. If the beam is not broken at a particular required frequency, the electron beam is shut down.

4.7.3 Dosimetry

Dosimetry is an important and necessary feature for all food irradiation facilities as it is vital in protecting the health and safety of the public. And as such, it is necessary that proper recording and measuring procedures are followed. This is also a necessary feature in the current regulatory and commissioning process.

A dosimeter food irradiation package would be designed to measure the dose at the maximum and minimum points in the package. This would be on both the front and back and in the middle. This would cover the minimum amount of dose received in the middle and maximums at both ends following flipping of the package. The device would be filled with strawberries as best as possible to emulate the actual settings. Perspex or radiochromic film dosimeters are typically used for their low cost. However alanine film dosimeters could also be used, but the high costs of the required readout component make them less desirable. All three types will produce accurate results at the 1 kGy level, but alanine film dosimeters appear to produce the best results[1]. All three dosimeter types also fit the size limitations.

The package would be run less frequently than would be required for gamma or x-ray sources. At a minimum the package should be run following each start up, but ideally,

for best records, the package could be run every hour. The readout component would be placed with the trailer. Results should be entered into an accompanying data acquisition system that could track all data. These records must be kept for a minimum of one year as per regulations. Package dose data could also be utilized in optimizing the irradiation of the food. The conveyor belt speed could be adjusted to increase/decrease the dose rates. The dosimeters will be required to be calibrated according to standards.

TLDs (Thermo Luminescent Dosimeters) would be used to monitor exposure to personnel. These detectors are common and well developed in this application. The doses measured from the TLDs will be logged and carefully monitored at a proper frequency, annually or semi-annually. Also included to protect the workers will be a no-entry zone 25 feet around the accelerator. This will be needed to ensure the minimum amount of dose allowed. This boundary will be well marked and monitored.

4.7.4 Access Door Interlock

A necessary safety feature would be an interlock. A safety interlock is a safety mechanism that will disconnect power to the accelerator if a hazardous condition arises. Interlocks on access doors are considered necessary at all irradiation facilities as exposure limits could be exceeded, and fatal exposures could occur. In this design access to the irradiator would not be fatal, but in order to reduce risks to as low as reasonably achievable, an entry interlock system would still be incorporated. This type of system could be designed in coordination with the accelerator manufacturer since it is fairly standard.

The basic function of the entry interlock is that all operation of the irradiator would stop if the access door was being attempted to be opened or if the interlock system

was malfunctioning. This could be operated with a key and digital system from the accelerator control system. Management or designated personnel would be the only people allowed to open the access door. Regardless of this, the opening of the door would stop the accelerator in case the appropriate procedures were bypassed. Accompanying this would be exterior and interior lights to signal the operation of the accelerator. Also on the interior of the entry point an emergency stop button would be placed as well as sirens and flashing lights some allotted time prior to start up. An emergency stop button will also be included on the exterior of the entry point as well on the control unit. These buttons will work separately from the control unit to ensure that malfunctions in the system will not interfere with these safety features. Lights would also be placed at the end of the maze points of the conveyor system.

4.7.5 External Generator

The generator would be placed outside of the irradiation Conex box area. It will be stationed during transport on a trailer behind the box. This would ensure that the electron accelerator could not receive any power during transportation.

4.7.6 Ground Sensor

An ideal safety feature would be an instrument that could ensure that the design is properly seated on ground level. This would be recommended since the ground is a primary shielding component in that it would be used to shield all radiation exiting from the bottom of the Conex box. One instrument that might accomplish this is an ultrasonic sensor. A benefit of ultrasonic range sensors is that it could be placed a certain distance

from the bottom of the unit. This differs from a bellow type design that would have to be placed on the bottom of the box and could potentially degrade after several loadings on and off the truck. Two or more of the sensors could be placed around the Conex box. Then upon startup the control systems would check to ensure that it is placed properly on flat ground.

4.7.7 Built-in Safety Features of the Accelerator

The linear accelerator can be customized in coordination with the manufacturer. This will include safety features directly associated with the accelerator. This will also include the control system which will be located outside the designed accelerator unit. The control system will display the status of all previously mentioned safety features.

4.7.8 Safety Features Summary

These safety functions could be classified into three types: safety of the workers and personnel, proper irradiation of the food, and ensuring that the design was placed properly on the ground. The most important safety function is to prohibit people from entering into the irradiation zones where the doses could be fatal. This design is able to limit people from entering the area based on the very small entry points into the irradiation zones. People are also limited from entering the accelerator area by using a single entry interlock. The design would also utilize emergency stop buttons inside and outside the entry point for workers to manually stop the accelerator in case of emergency. Workers would also be equipped with TLDs to monitor dose received. A 25 foot radius would also be placed around the facility perimeter.

The second group of safety features would ensure the proper irradiation of the food. The conveyor operation had to be monitored to ensure that products were not lodged and the speed of the belt was correct for irradiating with the proper dose. Dosimeters would occasionally be ran through and recorded properly.

The third group of safety features would be designed to ensure the Conex box was properly seated on the ground. The design runs off an external generator which would have to be setup following the unloading of the design. Then upon startup, the control systems would utilize sensors to determine if the box was properly seated on the ground.

Other safety features could be of interest in future research and design. The accelerator could be appropriately designed with the manufacturers to handle safety functions that pertain to its functionality.

Table 4.7.1: Cost of the Safety Features

Component	Costs ($)
3 Chromatic Dosimeters	2,550
Chromatic Readout	4,000
Calibration of Dosimeters	2,173
TLDs	100/per
Infrared Beam for Conveyor	50-150/per
Ultrasonic Range Sensor	50-150/per

4.8 Ozone

Ozone (O_3) can be created when photons interact with dioxygen (O_2) molecules. Dioxygen breaks apart into its individual oxygen (O) atoms, which have the potential to bond to other dioxygen molecules to form ozone. Ozone is common in the stratosphere, but is also known to exist in high concentrations in polluted areas on the surface of the Earth. Ozone itself is considered to be a form of pollution and is known to cause lung and cardiovascular diseases in those who are exposed to concentrations as small as 40 parts per billion[17]. These effects can be caused by short term (at a work site) or long term (environmental) exposure. Food irradiators are known to produce ozone, including sources such as Cobalt-60 and accelerators. In large-scale food irradiation facilities systems are used to remove ozone, but this is especially frustrating for the conceptual design of a compact, mobile irradiator. In this design, the food pathway from entrance to exit is solid and sealed for shielding purposes, which means that all ozone produced in this machine can flow either direction out of the electron beam target area and out of the entrance and exit ports for food. The production of ozone at such a machine would be relatively small in comparison to a large-scale permanent facility, and the open-air conditions would prevent the ozone from accumulating around workers. Workers would be near the food ports, however, loading and unloading trays. These are points of concern, so an internal ventilation system has been devised to move gas from the food pathway to a high point on the far end of the machine. Air ducts are to be placed near either food entrance, leading from the top of the pathway to a safer exit point. This is to eliminate unnecessary penetrations in the shielding close to the target area. At all times of operation, air will be forced from the internal ducts to the far end of the machine. This will suck air from the outside, minimizing the leakage of ozone near workers, while a

small fume hood and curtains hang over the wall penetrations for added safety. The OSHA permissible exposure limit is an average of 0.1 parts per million over an 8 hour work period[18]. Ozone detectors are readily available for a few hundred dollars and can be used near the side wall penetrations for safety purposes[19].

The safety systems to minimize ozone exposure to workers are as follows:

1. Internal air ventilation that sucks air from the outside, though the wall penetrations and leads to a high point outside the machine further away from workers.

2. Small fume hoods and flaps near wall penetrations.

3. Electronic ozone concentration detectors at all sites where workers are present.

5.0 Shielding/ Dose Analysis

5.1 Shielding

Characterization of the Photon Flux

For an e-beam source, characterization of the flux is inherently difficult due to the spectrum of energies created from the electron impinging upon the various target materials present during operation. A simplified problem geometry with a polyethylene target, Figure 5.1.1, was created to tally the photon flux as a function of energy. The

result is presented in Figure 5.1.2 below. In the Figure, blue is polyethylene, yellow is

lead, green is steel, aqua is air, and red is soil.
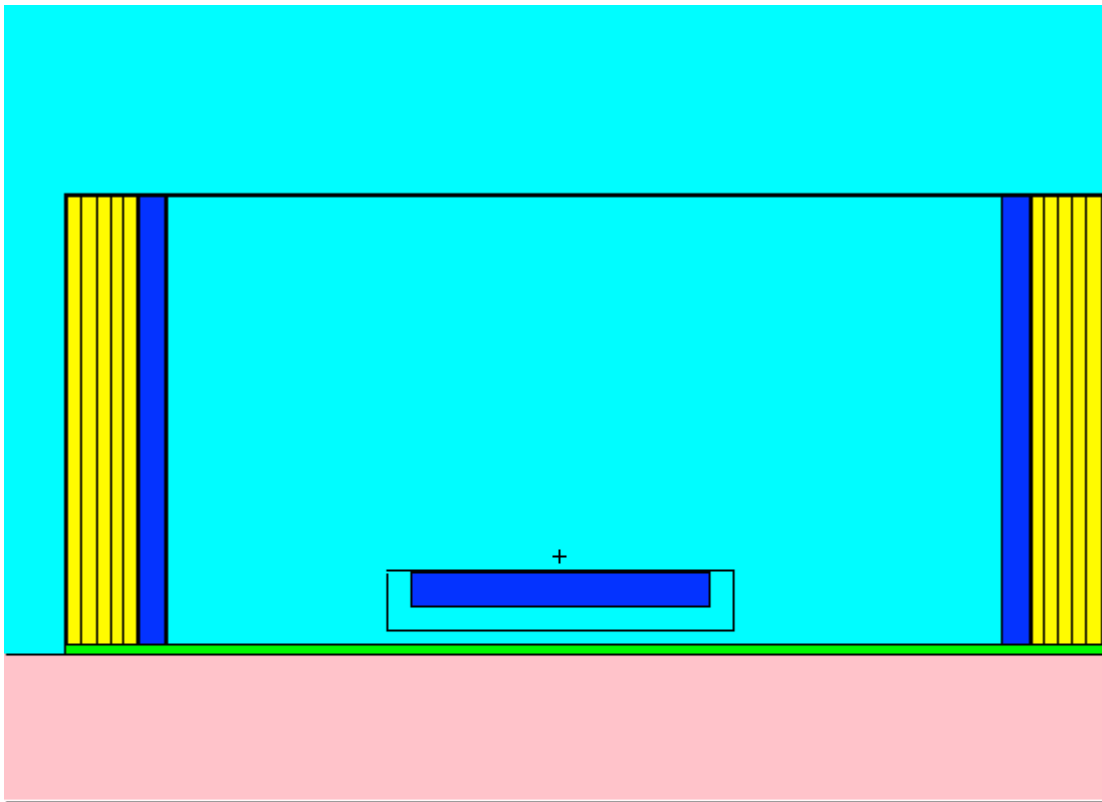
Figure 5.1.1: MCNP5 model used to characterize thick target bremsstrahlung spectrum

in polyethylene. Plus sign indicates the position of the 10 MeV beam. (Cut in x-z plane)
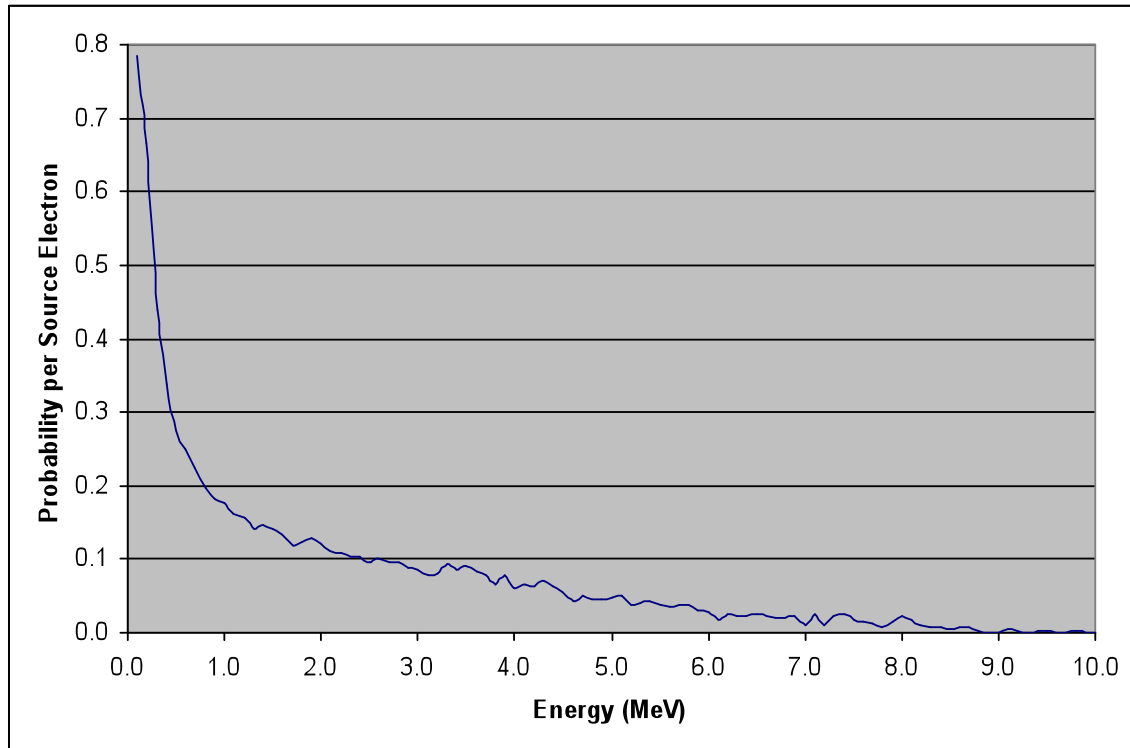
Figure 5.1.2: Thick target Bremsstrahlung spectrum for 10 MeV electron beam in

polyethylene

While characterizing the photon flux in this simple geometry is useful, it doesn't lend itself to a quick hand calculation of the necessary shielding. Additionally, it doesn't take into account the other materials that will be present in the actual shield thereby altering the distribution. Also, the presence of strawberries or other produce on the conveyor will also alter the characteristic distribution. Finally, due to the complex actual shield geometries, MCNP5 was unable to calculate surface area or volume of cells in the shield making it impossible to tally flux across any of the actual surfaces instead of a simplified model. Therefore, it is difficult to use a multi-group calculation that will be all encompassing for the various fluxes without several simulations being run to determine the worst possible flux to be seen in the shield. Considering that there is a better

36

alternative to give an upper estimate on the shield necessary, the half value layer (HVL) method is used instead.

Hand Calculation Using HVL:

The HVL is a useful tool for estimating the thickness of shield needed due to an electron source impinging upon a target. These values are tabulated and used regularly to estimate the shield necessary for x-ray machines. Although these values are based on x-ray machines which typically use a high Z target, it will provide an upper bound on the necessary lead thickness needed. For a 10 MeV e-beam, the HVL in lead is 16.6 mm[1]. To calculate the thickness of shield necessary, the desired dose at the work station, where the strawberries will be loaded and unloaded, must be calculated. Assuming 50wks per year, 8hr workdays, and a maximum exposure of 5 Rem/yr, the hourly exposure can be calculated as follows:

$X =$ (5 Rem/yr) * (yr/50wk) * (wk/5days) * (day/8hr) $= 2.5*10^{-3}$ Rem/hr

Additionally, the unshielded dose must be calculated. According to the manufacturer, this is ~1000 Rem/min at 1m (See Appendix I). Since we are only using 1/5 of the maximum 1kW power, calculations shown in the food analysis section, the unshielded dose can be estimated at 12,000 Rem/hr. With these values, the thickness of the shield can be calculated using the following formula:

$$\frac{D_{sh}}{D_{un}} = (0.5)^{T/HVL}$$

$T = \ln (D_{sh}/D_{un}) * HVL / \ln(0.5)$
$T = \ln (2.5*10^{-3} / 60000) * 1.66cm / \ln(0.5) = 40.69cm$ of lead for 60,000 Rem/hr
$T = \ln (2.5*10^{-3} / 12000) * 1.66cm / \ln(0.5) = 36.84cm$ of lead for 12,000 Rem/hr

This shield estimate of 36.84cm of lead was used in the initial designs of the shield to provide a starting point for shield thickness. Actual thickness in the shield will

vary to accommodate the unique design, unique thick target bremsstrahlung spectrum, and to reduce overall weight to approach a reasonable size for mobility purposes. Additionally, since the proposed design utilizes a low Z material as the primary beam stop, the majority of the bremsstrahlung will be forward peaked[20]. Therefore, there will be lower dose rates on the sides and top where the design calls for shielding (the ground serves as the bottom shield), and this method of hand calculation will tend to overestimate the actual shield needed for the top and sides due to the lower fluxes at these points.

Shielding Design:

Several designs were considered to provide the primary shielding. A couple designs that were tested but rejected are described below to show the evolution process that identified and refined important aspects of shielding requirements for a mobile food irradiator.

1) A large container, 20'x8'x8', completely shielded at the necessary thickness on 5 sides, the same truck design that allowed the bottom to be unshielded was used, with partially shielded conveyor entrances utilizing a drop zone and distance to minimize the solid angle for streaming photons. This design was simple and promising; however, the sheer weight of lead required to shield this size of container made this an undesirable approach to a mobile food irradiator. The weight of the shield, assuming 1' thickness of lead easily exceeds 425,000 lbs pushing the system weight to nearly 475,000lbs – clearly far too heavy to be mobile.

2) A smaller container, 8'x8'x6', shielded as described above utilizing the same conveyor entrance. This design suffered not only from excessive weight, ~180,000 lbs at 1' shield thickness, but also from difficulties with conveyor entrance and confinement issues – maintenance would be next to impossible.

3) A 10'x10'x7' container with a shielded conveyor, see Figures 5.1.3 and 5.1.4, utilizing two bends to minimize streaming effects. This design drastically reduces the mass needed to shield the food irradiation facility. In addition to taking advantage of placement on the ground, the conveyor is lowered to ~3.25" at the bottom of the conveyor to reduce shield height. This also lowers the ground scatter concerns that were present with elevated conveyor designs. The electron beam is fed into the shielded conveyor assembly through an imbedded scan horn thus limiting the opening in the top of the shield. While weight will still be an issue, streaming effects were not eliminated by two bends totaling 180º. Figure 5.1.5 demonstrates the expected dose rate in a 100'x50'x6' area on the side of the Conex using this design.
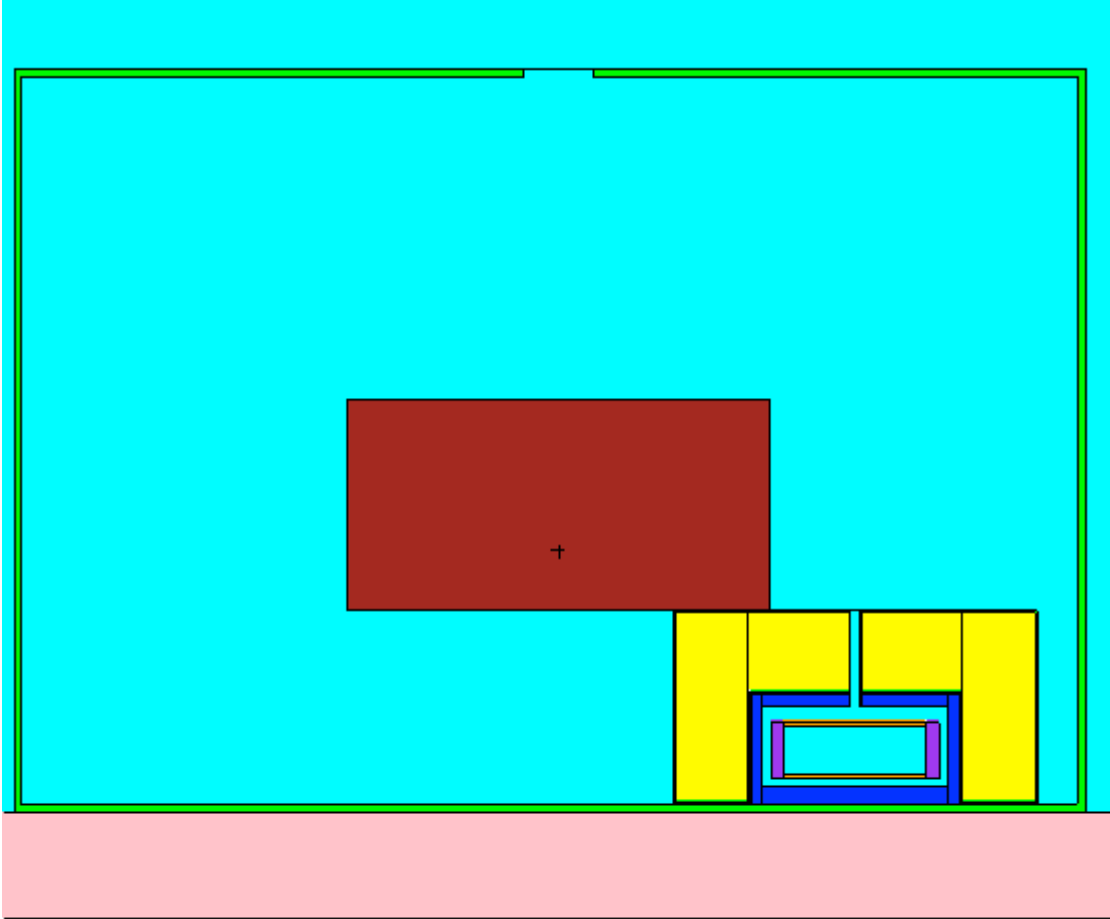
Figure 5.1.3: MCNP model of design #3. Green is steel, yellow is lead, blue is polyethylene, orange is the Delrin conveyor belt, purple is the conveyor sides, and aqua is air. (Cut in X-Z plane)
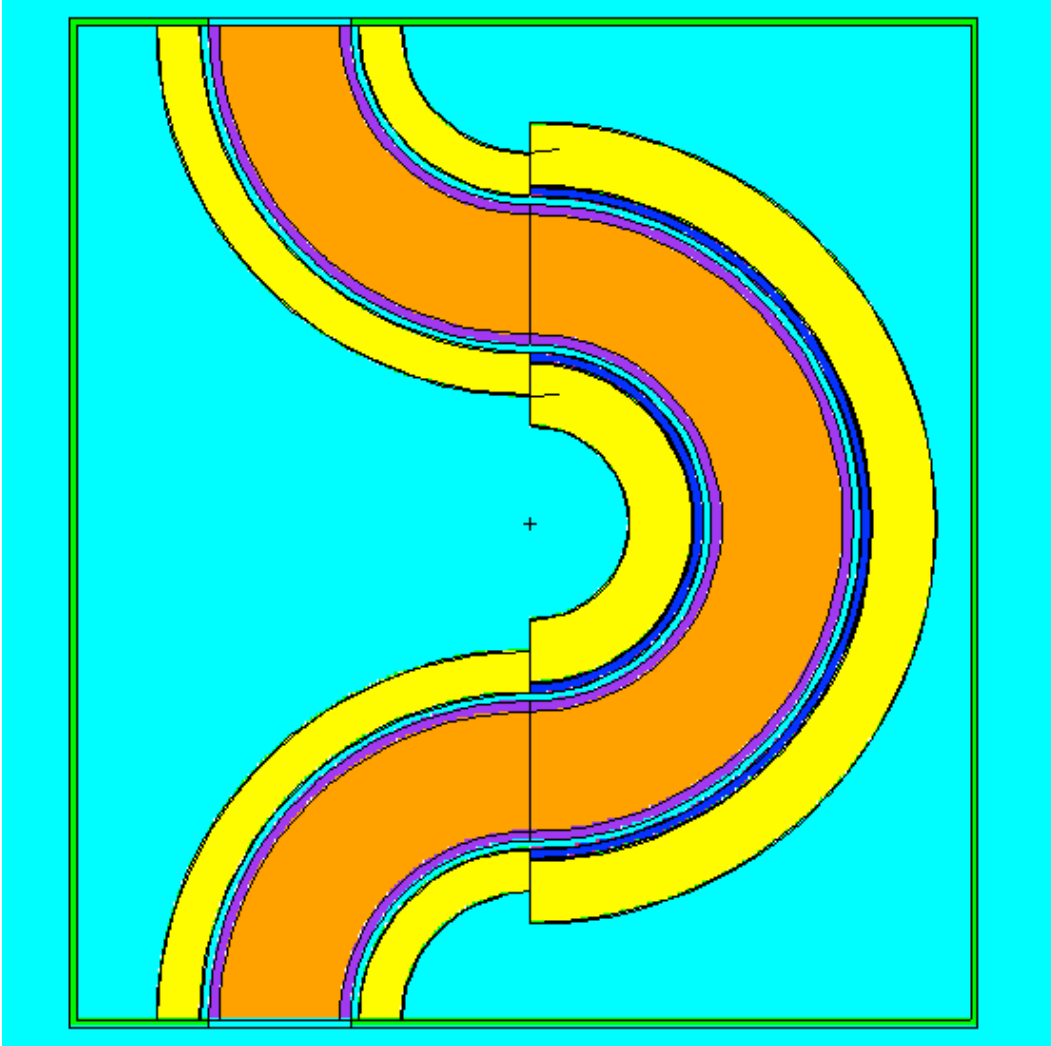
Figure 5.1.4: MCNP model of design #3 showing shielded 2-curve design. Green is steel, yellow is lead, blue is polyethylene, orange is the Delrin conveyor belt, purple is the conveyor sides, and aqua is air. (Cut in X-Y plane)

−198.12
−320.04
−441.96
−563.88
−685.8
−807.72
−929.64
−1051.56
−1173.48
−1295.4
−1417.32
−1539.24
−1661.16

−1648.32
−1404.48
−1160.64
−916.8
−672.96
−429.12
−185.28
58.56
302.4
546.24
790.08
1033.92
1277.76
1521.6

2.00E+02-2.05E+02
1.95E+02-2.00E+02
1.90E+02-1.95E+02
1.85E+02-1.90E+02
1.80E+02-1.85E+02
1.75E+02-1.80E+02
1.70E+02-1.75E+02
1.65E+02-1.70E+02
1.60E+02-1.65E+02
1.55E+02-1.60E+02
1.50E+02-1.55E+02
1.45E+02-1.50E+02
1.40E+02-1.45E+02
1.35E+02-1.40E+02
1.30E+02-1.35E+02
1.25E+02-1.30E+02
1.20E+02-1.25E+02
1.15E+02-1.20E+02
1.10E+02-1.15E+02
1.05E+02-1.10E+02
1.00E+02-1.05E+02
9.50E+01-1.00E+02
9.00E+01-9.50E+01
8.50E+01-9.00E+01
8.00E+01-8.50E+01
7.50E+01-8.00E+01
7.00E+01-7.50E+01
6.50E+01-7.00E+01
6.00E+01-6.50E+01
5.50E+01-6.00E+01
4.50E+01-5.00E+01
4.00E+01-4.50E+01
3.50E+01-4.00E+01
3.00E+01-3.50E+01
2.50E+01-3.00E+01
2.00E+01-2.50E+01
1.50E+01-2.00E+01
1.00E+01-1.50E+01
5.00E+00-1.00E+01
0.00E+00-5.00E+00

Figure 5.1.5: Dose rate mesh tally demonstrating streaming issues with design #3. The origin of the stream at the top of the figure corresponds to the coordinates of the opening for the conveyor. Dose rates are in Rem/hr and vary from 0-20.5 Rem/hr.

4) After identifying streaming issues, ground scatter issues, and weight concerns as the primary issues with the shield design, an S-shaped curve with very little top shield, 1cm of steel, was used. The cross section of this design is shown in Figure 5.1.6 below.
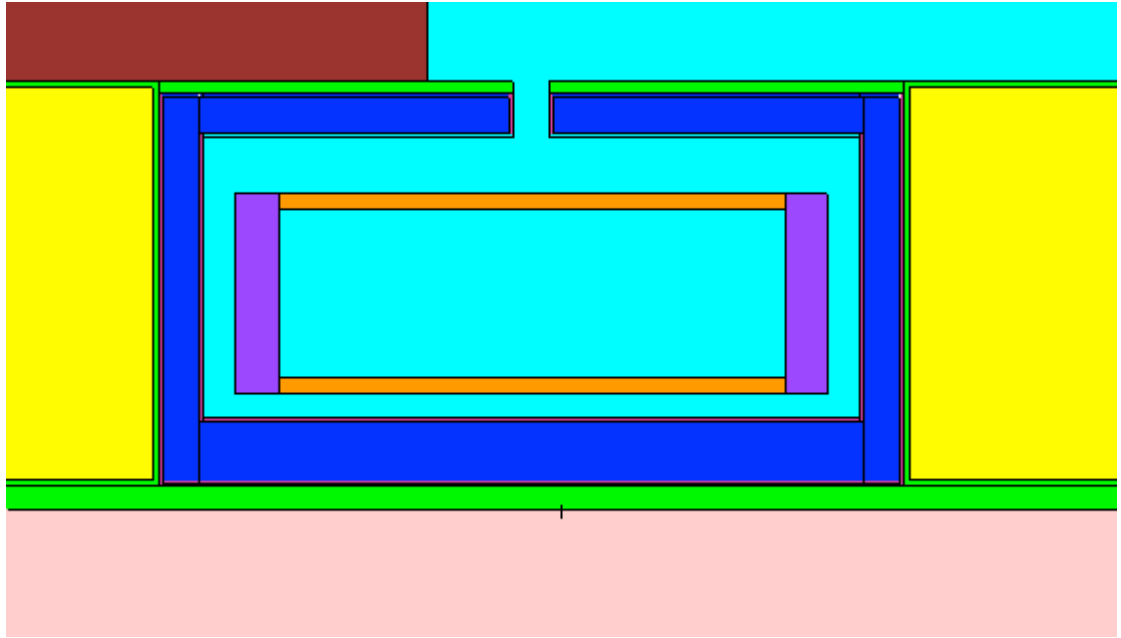
Figure 5.1.7: Cutaway of proposed conveyor shield design (Cut in X-Z plane). See Table 5.1.1 below for color-material correspondence.

This design drastically reduced weight, ~28.5k lbs, but suffered from scattering issues at the top of the container. Initial thoughts focus on the lack of skyshine being an issue for radiation to personnel. However, due to low side shield heights, the flux through the top was not as collimated as would be desirable. Additionally, low energy photons, those more likely to scatter, escape the shield containment and san scatter from the CONEX container. These scattered photons then contribute to personnel dose. This was the same issue identified earlier with ground scatter. With a large distance between the photon origin and the absorbing medium (or in the air's case a largely non-scattering medium), photons are more likely to scatter and then contribute to personnel dose. These competing issues make it impossible to place the

43

conveyor and side shield in any location that would both minimize the side shield height and reduce issues related to scattering. Figure 5.1.8-9 below shows the dose rates obtained from the MCNP5 simulation with a small top shield. As can be seen from the graphs, dose rates outside the CONEX are on the order of 100-300 times larger than when a large shield top is used.
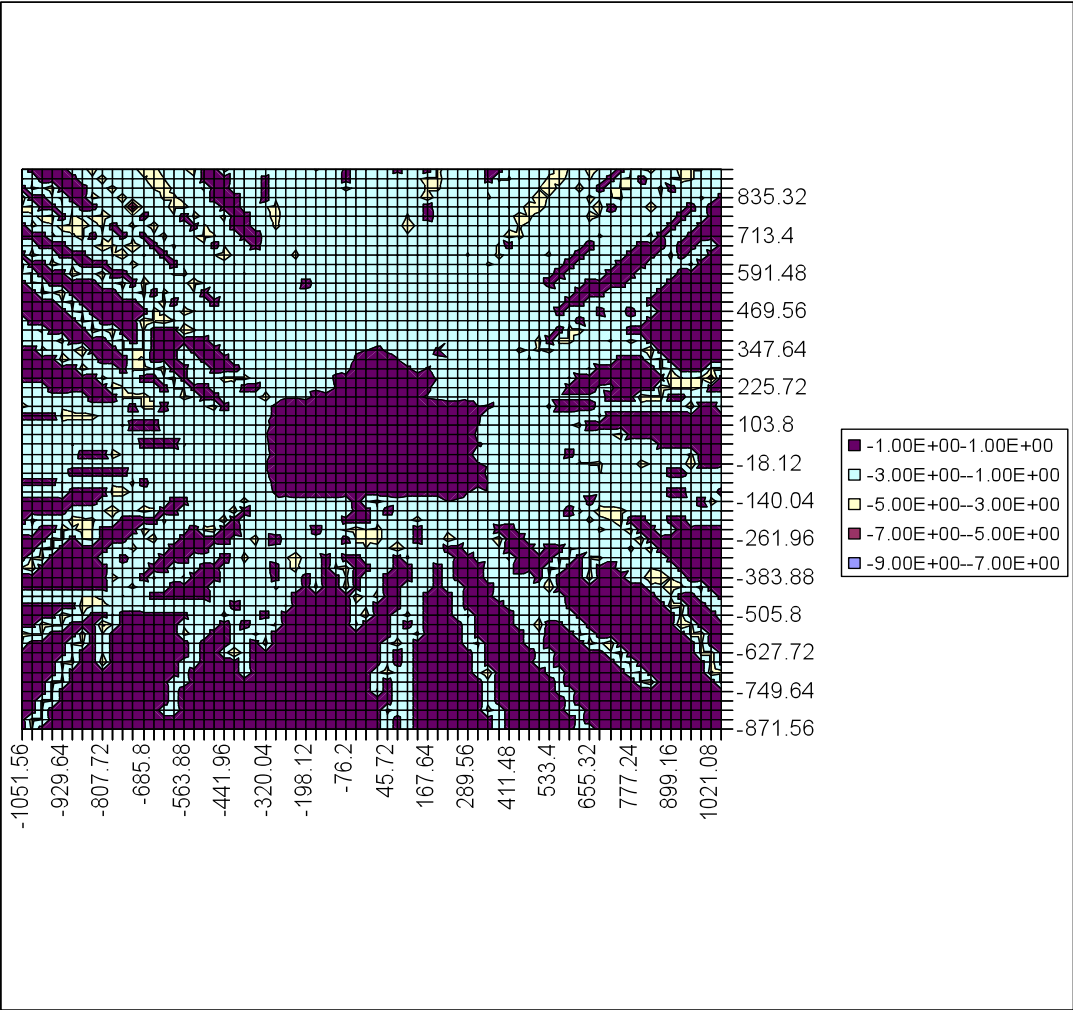
Figure 5.1.8:Log dose rate plot utilizing 1cm top shield. Values are in Rem/hr. This plot shows that a significant dose is delivered everywhere in a 25' radius around the container. While illustrating that a dose is delivered everywhere, Figure 5.1.9 is better for reading values and seeing high dose rates.
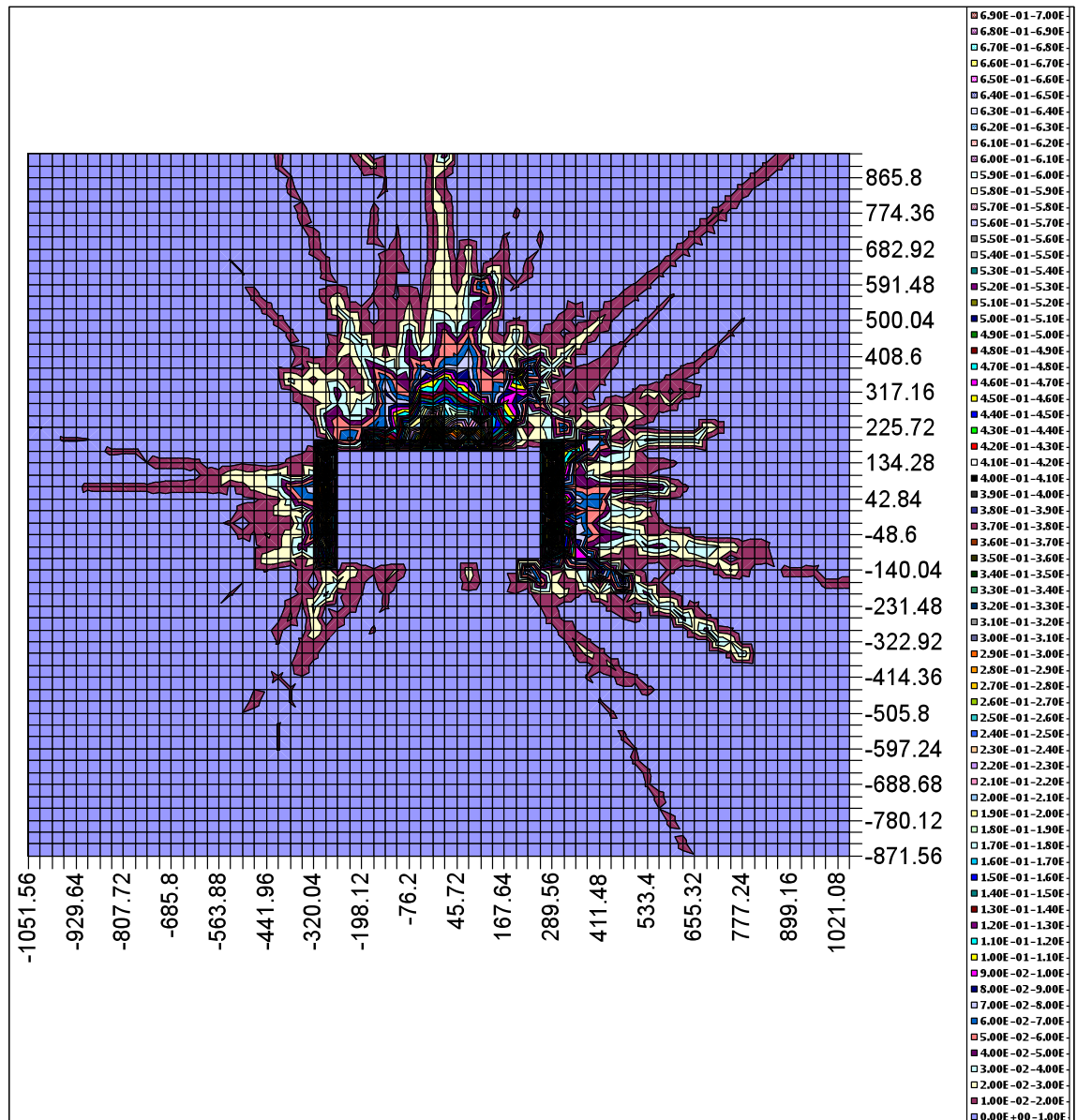
Figure 5.1.9: Dose rate plot utilizing 1cm top shield. Values are in Rem/hr. This plot

shows that a significant dose is delivered outside the container. The rates, difficult to

see, range from under 0.01Rem/hr in blue (4 times the desired dose rate) to 0.7Rem/hr

close to the CONEX. Rates on the edge of the 25' exclusion zone range as high as 0.0876

Rem/hr (35 times the desired dose rate).

Final Design and MCNP Model:

After testing and rejecting the above designs, the design shown is Figure 5.1.10 was chosen as the final design. For all of the MCNP models presented in this section, Table 5.1.1 shows the color to material correspondence.
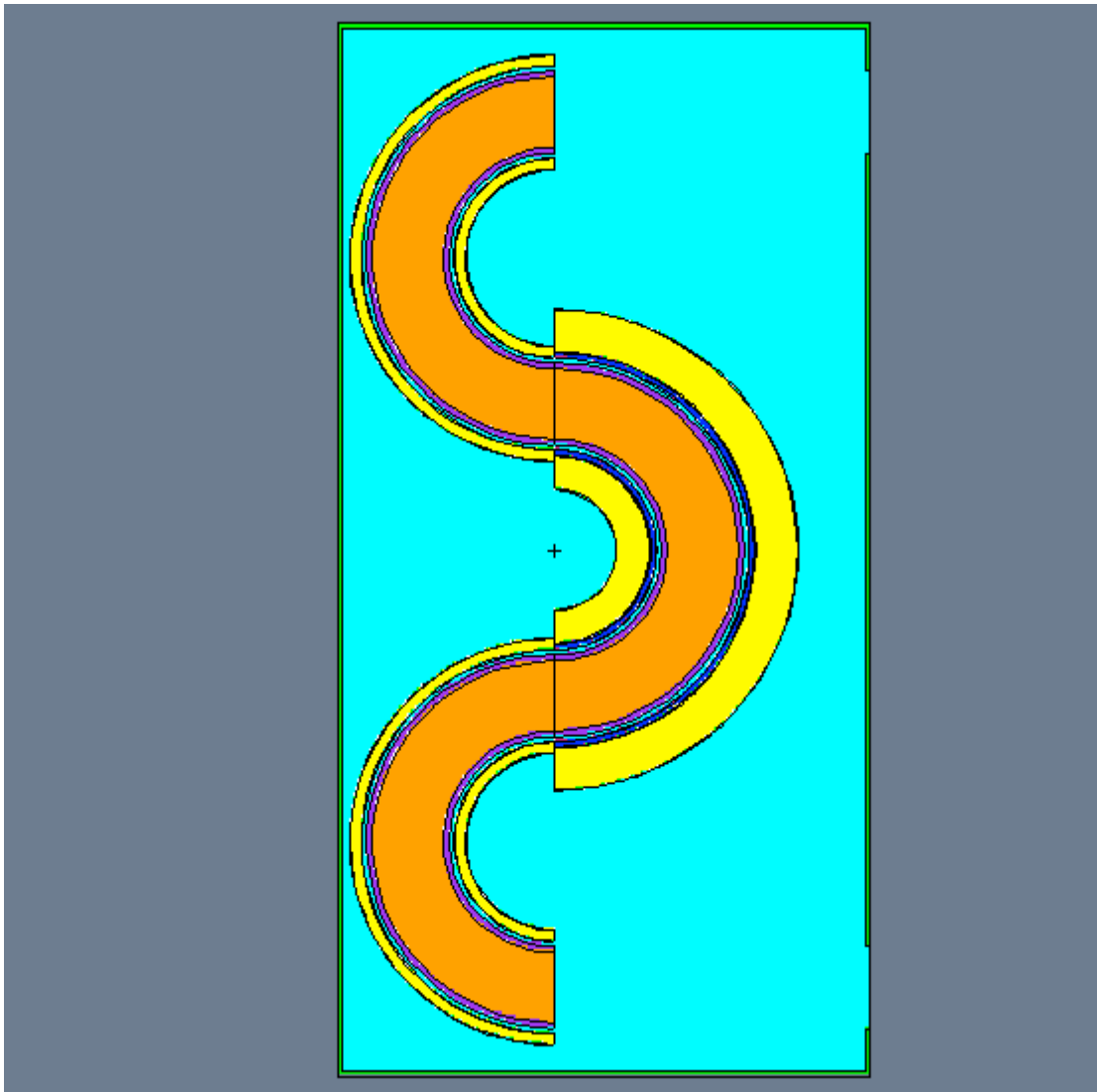
Figure 5.1.10: MCNP Model of final shielding design (Cut in x-Y plane).

Table 5.1.1 – Material Correspondence for MCNP5 plots

Color	Blue	Orange	Purple	Yellow	Green	Aqua	Red	Pink	Grey
Material	Poly	Delrin	Al/Poly	Lead	Steel	Air	Al	Soil	Water

Material compositions for each are shown in the MCNP deck used for shielding calculations in Appendix III. Input parameters used for the run are also shown in Appendix III.

The S-shape design allows for conveyor entrance into a relatively small volume while eliminating streaming effects due to scattered photons that were the primary dose rate contributors in previous designs rejected above. Although this increases the size and weight of the shield, it was by far the lowest for any shield design considered and an unavoidable step necessary to reduce streaming photons trough conveyor entrances. Additionally, by eliminating streaming effects, geometric attenuation can be used to further reduce the dose rates seen on the outside of the shield as will be described later. This was not as useful when streaming effects were large due to the narrow path that the scattered photons were traveling on. This effect can be seen on the dose rate graph in Figure 5.1.5 above in the rejected designs region.

The shield is designed as described above in the general design concept section. Figure 5.1.11 shows a sample cutaway from a point in the shield.
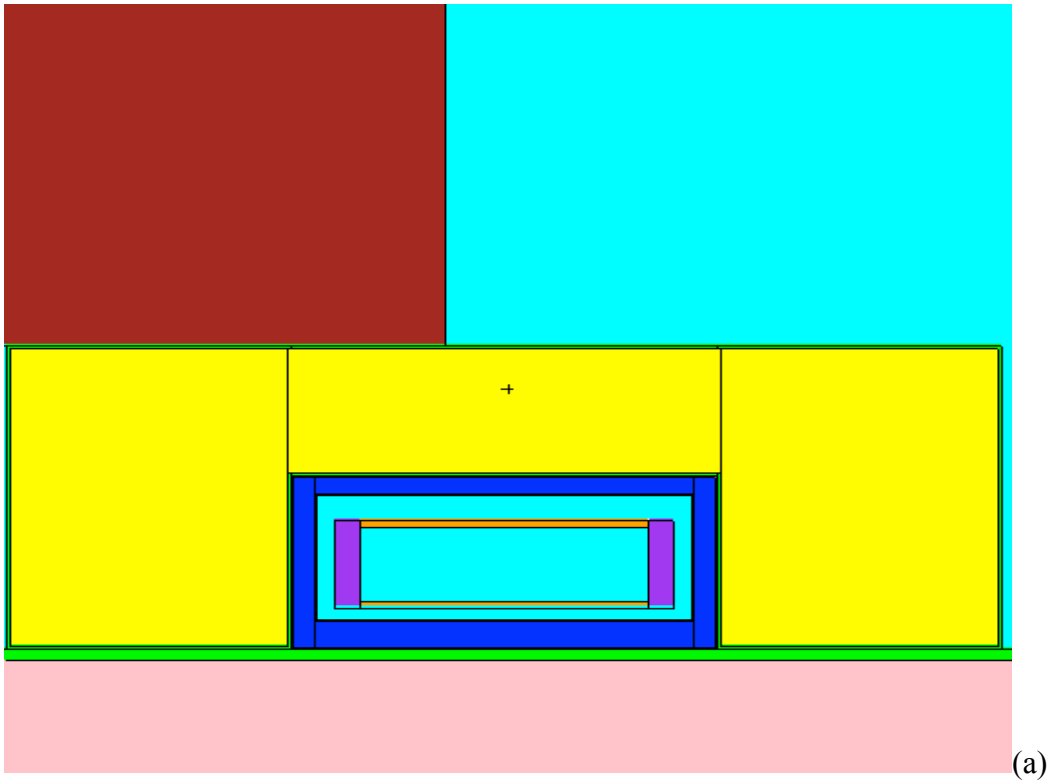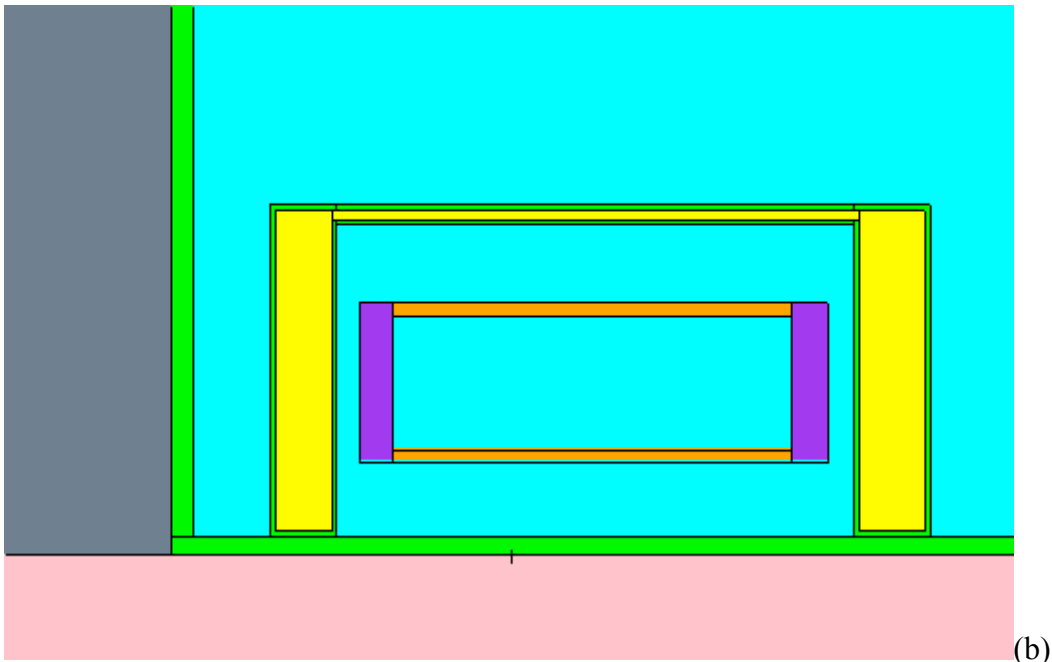
Figure 5.1.11: Cutaway of conveyor shield design (Cut in X-Z plane). (a) is cutaway of main conveyor shield. (b) is cutaway of secondary streaming shield.

The polyethylene is thinner on the top and sides, 3cm vs. 5cm, due to the directional nature of the electron source. However, due to scattering and the strong dependence of the bremsstrahlung spectrum on Z (computer simulations showed that the flux and average energy increased by a factor of ~2.3 when aluminum was used as a beam stop vs. poly), poly was still necessary on the sides and top to reduce the lead shielding necessary for the radiative photons generated from the electrons. As described above, all polyethylene is encapsulated in a thin 0.25cm aluminum casing to combat material deformation due to the high radiative flux.

The conveyor modeled has two Delrin belts with sides made of an aluminum and polyethylene composite. This conveyor mirrors the one described above in previous sections[22]. The conveyor is placed low to the ground to minimize the shield size and the scatter of photons back into the work area as noted in the failed design section.

The lead shield is of varying thicknesses to minimize weight while maximizing protection and keeping ALARA in effect. The lead is also encapsulated in a 0.5cm layer of steel to combat lead creep and biological concerns. Table 5.1.2 below describes the various thicknesses of lead shield used. These thicknesses are less than the hand calculated dose rate above for several reasons. First, the forward peaked nature of the bremsstrahlung radiation provides for a much smaller dose rate on the sides of the conveyor than would be present at the bottom. Second, the inner curvature benefits from geometry allowing for a smaller width (See Figure 5.1.10 above). Finally, the top shield is solely designed to stop a majority of the low energy photon flux to reduce scattering concerns outside the shield (high energy photons occur less frequently and are less likely to scatter) as identified above. Since the dose rate into the sky is not important to control

for personnel protection, mere geometric attenuation will suffice for reduction of the dose rate due to the collimated photons escaping the shield. However, precautions must be taken to ensure no personnel are on top of the CONEX during operation (the 25' exclusion zone accomplishes this).

Table 5.1.2: Thicknesses of the lead shield at various points in cm

Location	Outer Main Curvature	Inner Main Curvature	Main Top	Outer Secondary Curvature	Inner Secondary Curvature	Secondary Top
Thickness (cm)	25	20	10	7	7	2

The container modeled was a standard ISO Conex described in previous sections. It had two holes of the minimum possible size, 47.68cm x 14.67cm, to allow for conveyor entrance/exit points. Additionally, there is a cutaway in the top to allow for ventilation as described in previous sections.

The 5'x3'x3' e-beam head was also modeled due to its size. However, it had minimal photon interaction throughout its volume and contributed little, if any, to the shielding.

Shielding Dose Rate Analysis:

The dose rate was calculated throughout a 120'x110'x6' volume plus additional calculations for the dose rate at the top of the container. This was accomplished with an F4 mesh tally in MCNP5 that subdivided the area into 1'x1'x6' elements. A flux to dose conversion was accomplished through the values provided in Table D.3 for photon dose

on anthropomorphic phantoms[20].   The anteroposterior conversion was chosen as the worst case scenario (highest flux-to-dose conversion factors).   Water was chosen as a suitable substitute for anthropomorphic phantoms. Additionally, the value was multiplied by the number of particles produced by the e-beam in 1hr, 4.49×10^{17} and a factor of 100 to convert from Sv to Rem for a total multiplier of 4.49×10^{19} through a card to normalize the output to provide the dose rate in Rem/hr. The input deck used is included in Appendix III. An abbreviated output file is included in Appendix IV. The complete output file and mesh tally output could not be included due to size and bulk; however, pertinent results are presented below and in Appendix IV.

Variance reduction was used to be able to produce results in a reasonable time frame (See Appendix III). Due to the high particle flux, 1.25×10^{14} e/sec, it is impossible to simulate the number of particles that occur in any reasonable time span. The BBREM card and cell splitting help combat this issue and provide for more realistic results with fewer particles. Even with these methods, 10,000,000 particles were run for a total run time of ~93hrs. Despite all of these measures, the relative errors seen outside the shield, see Figure 5.1.12 below, were still unacceptable and > the standard 10% acceptability level. This could be improved by a longer runs on better computers and improved variance reduction methods, but it would require a long dedicated run to drastically improve the statistics at the edges where the calculated dose rate is most important for personnel considerations. Figure 5.1.12 shows, perhaps better than the following dose rate figures due to the smaller variation in the relative error as compared to the several order of magnitude variation of the dose rate, the areas where there was a dose delivered outside of the shield. Additionally, the horseshoe shape in the center highlights the main

51

shielded area, where the statistics were good, rather well. Light blue does not mean that there was no dose deposited, but rather that if there was a dose deposited, the relative error was below 25%, which is relatively acceptable with the limitations faced.
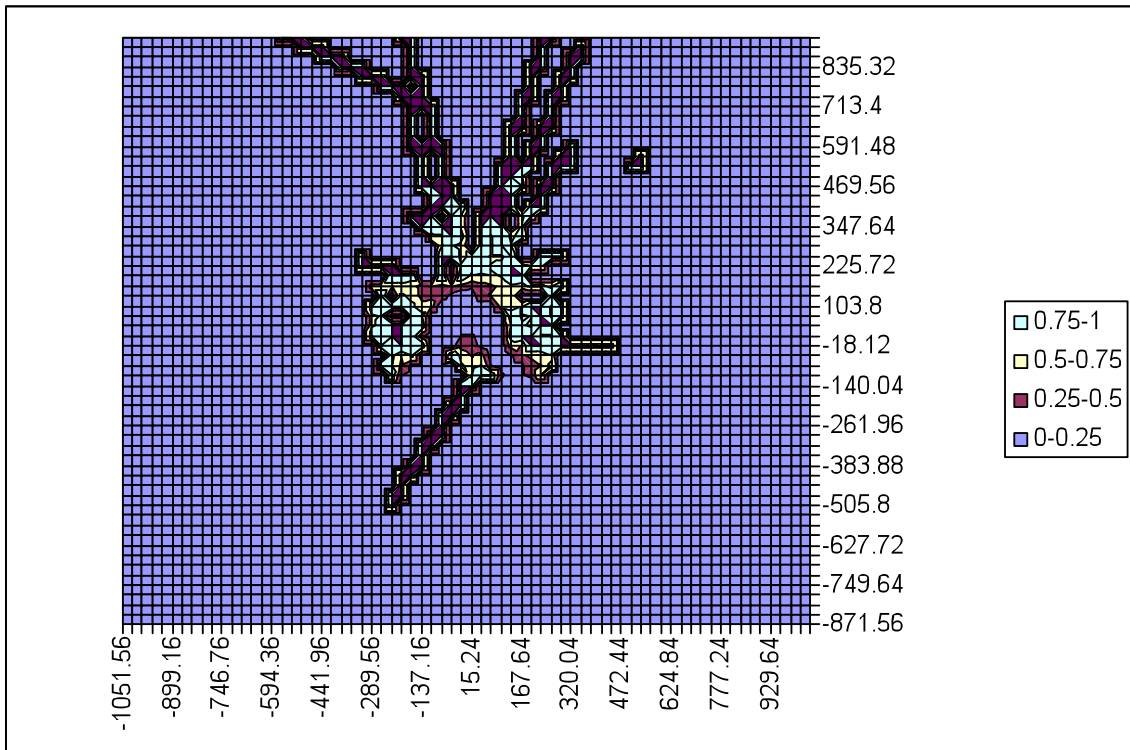
Figure 5.1.12: Relative error plot of the 70' x 60' x 6' area monitored for dose deposition.

The dose rate results obtained from the mesh tallies are displayed in Figures 5.1.13– 5.1.15 below. Figure 5.1.13 shows the entire 70' x 60' x 6' tally volume. Figure 5.1.14 shows the dose rate on the inside of the Conex box. Figure 5.1.15 shows the dose rate experienced on the outside of the Conex.
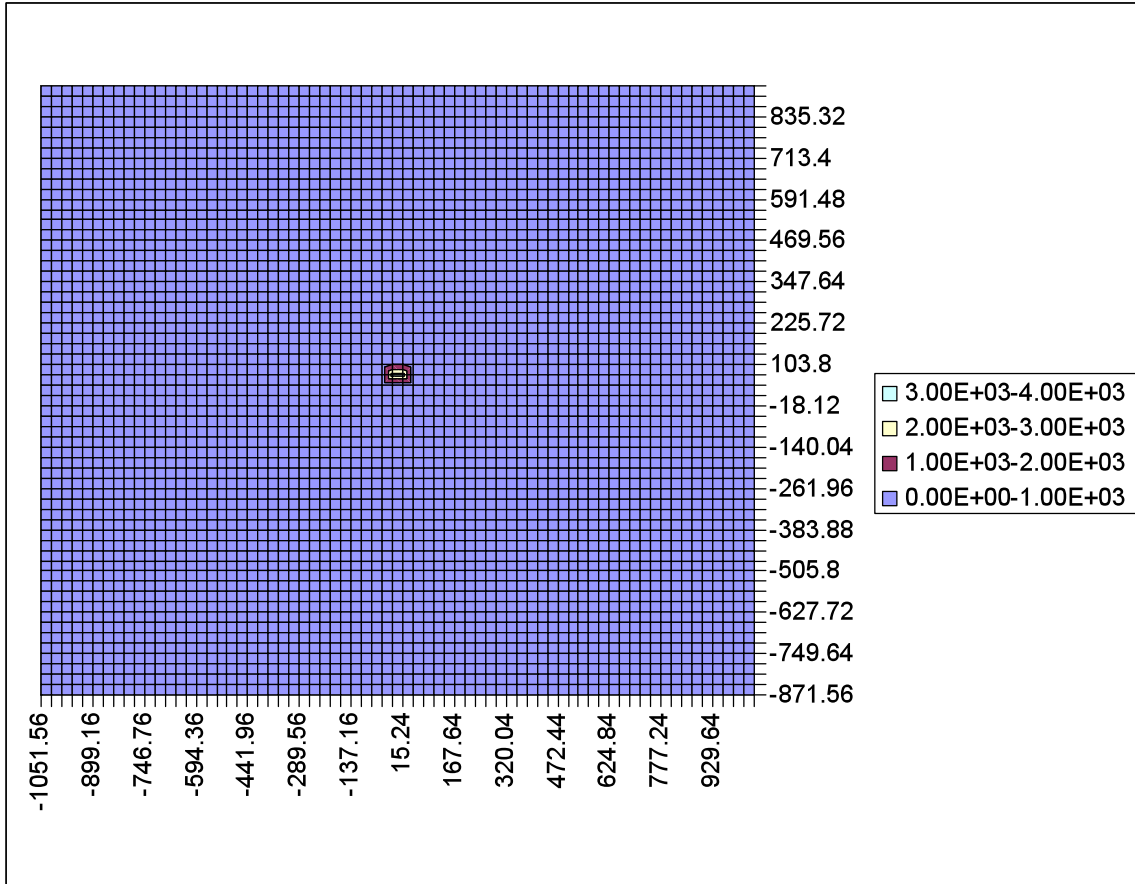
Figure 5.1.13: Dose rate in 70' x 60' x 6' Volume centered on CONEX. Rates shown are

in Rem/hr.

As can be seen from this figure, the primary dose deposition occurs inside the confines of the CONEX. In fact, the dose seen is confined to a small portion of the shielded area to the large variations, ~8 orders of magnitude from the inside of the shield to the 25' monitored boundary. To more accurately show the dose rates in the Conex, this section is shown in Figure 5.1.14 below.
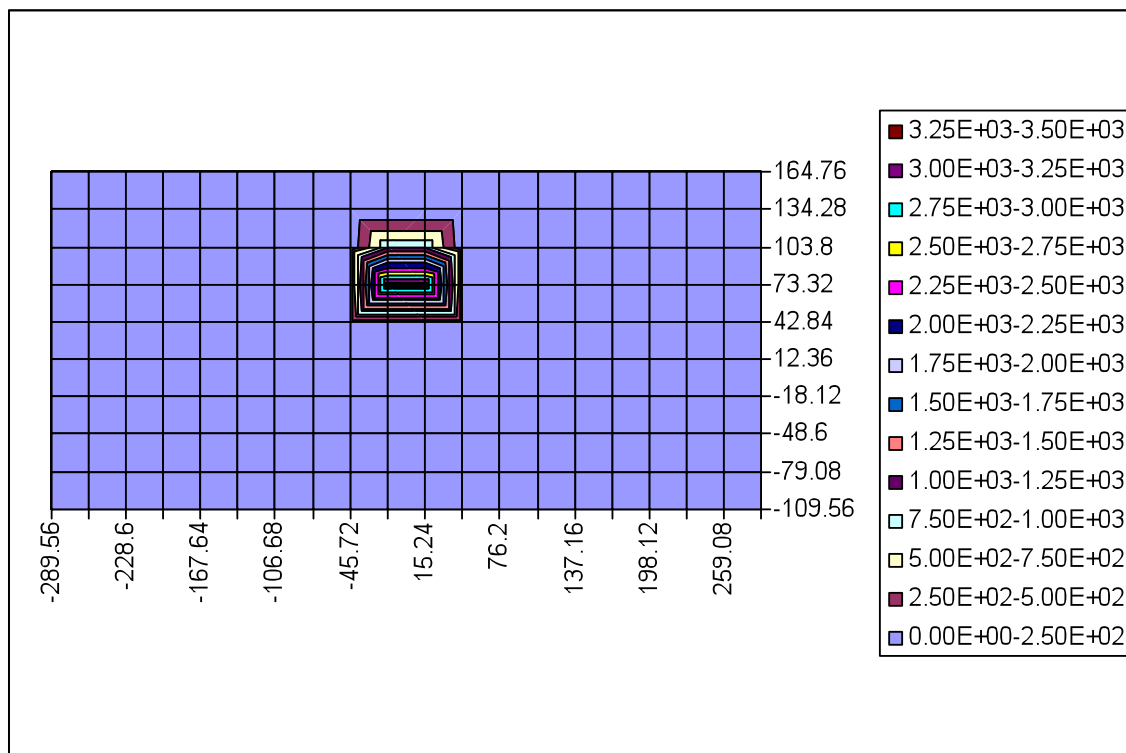
Figure 5.1.14: Dose Rates in CONEX. Rates are in Rem/hr. Area shown constitutes the boundary of the CONEX box with the primary dose deposition area being only a fraction of the total volume.

This figure, while slightly misleading due to washout in other cells from the concentrated high rates, shows that the majority of the dose is deposited in a relatively small area, ~4'x4', centered on the beam. It is worth noting that all of there area shown in the figure is within the CONEX walls. Therefore, it also shows that the majority of the dose is deposited well within the walls of the container minimizing the number of photons that scatter from the soil or CONEX wall directly into the air outside the containment volume of the CONEX. This was an issue faced in previous designs when the front edge of the shield was placed as close as possible to the edge of the CONEX. In this design, the beam was moved as close as possible to the center of the CONEX to

minimize this effect – see Figure 5.1.6. Figure 5.1.15 below shows the dose rates outside the CONEX perimeter.
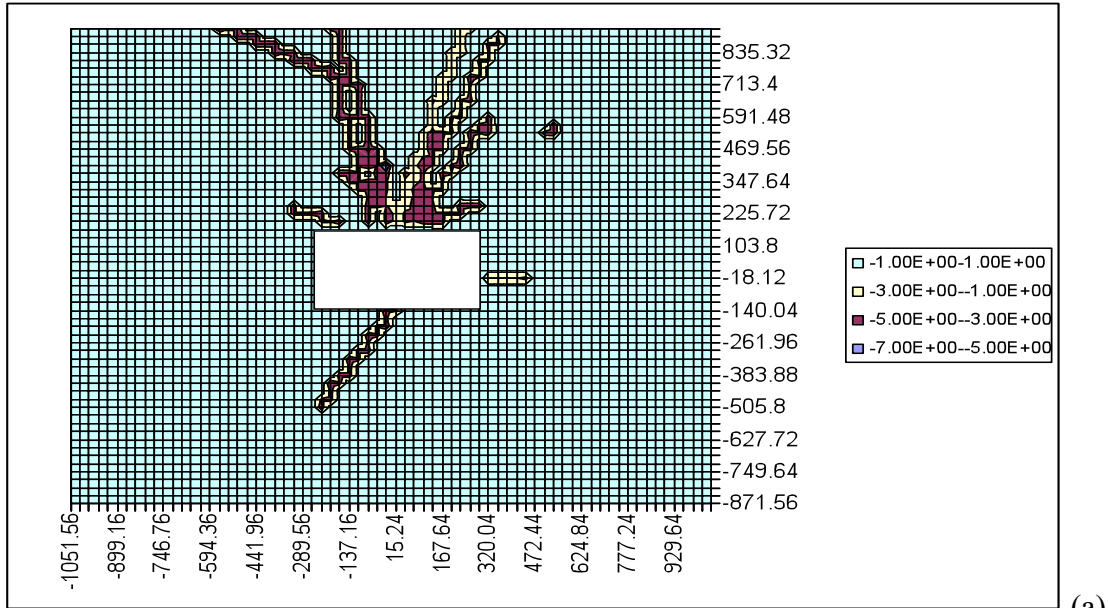
(a)
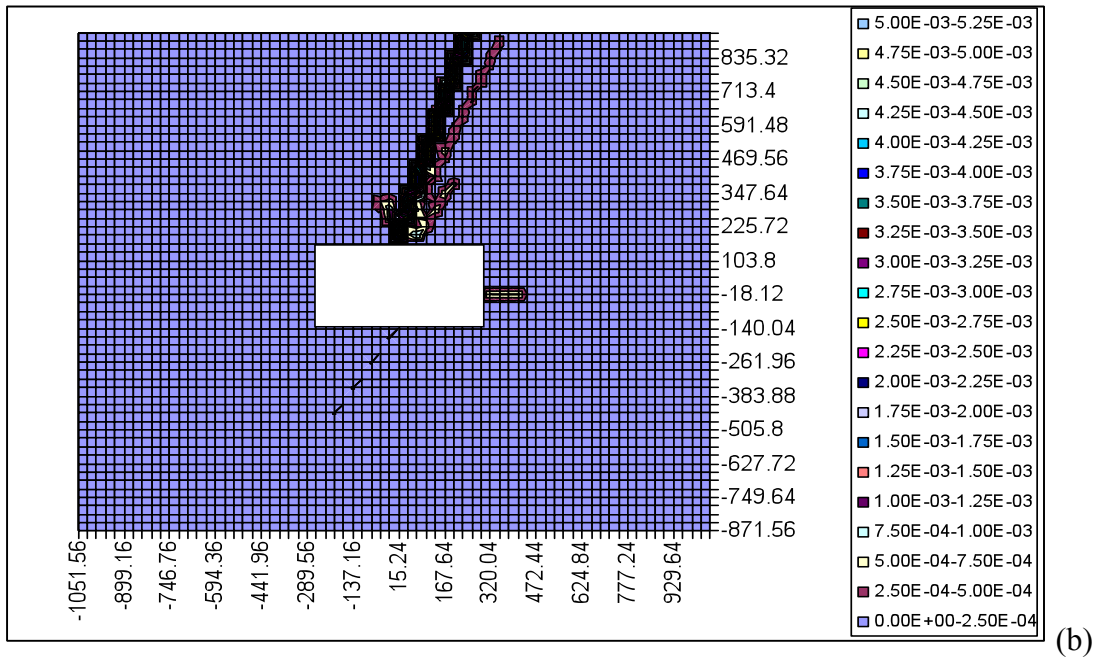
(b)

Figure 5.1.15: Dose Rate Outside of Conex. White Box represents the Conex boundaries. Rates are in Rem/hr. (a) Shows the dose rates on a log scale. (b) Shows the Dose rates on a linear scale. Outer edges of plot are 25' from edge of CONEX.

This figure shows the dose rate from photons that escape containment. The rates, although above the 2.5mRem/hr threshold at the edge of the Conex, are quickly attenuated to below that threshold due to geometric attenuation and are well below at the 25' administrative processing boundary established. This plot shows that the primary dose occurs from directly behind the beam through the outer main shielding. This is not to say that there is no dose through other areas, but instead, due to variations of 3 orders of magnitude, these are essentially washed out from the above plot. However, all of these are well below the 2.5mRem standard needed to satisfy occupational dose limitations. To better see the rates in the region behind the Conex, this area is expanded in Figure 5.1.16 below.
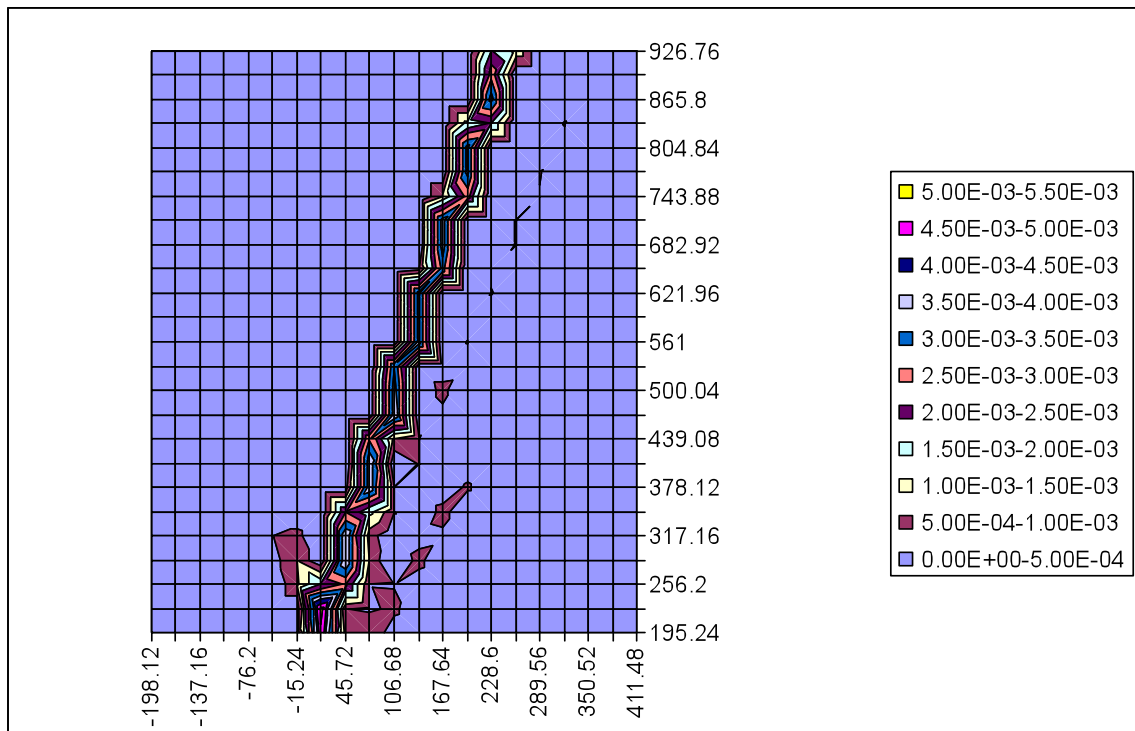
Figure 5.1.16: Dose Rate Outside of Outer Main Shielding in Rem/hr.

Although not readily apparent from the figure, the maximum dose rate received on the outer 25' mark is 2.05mRem. Although this is below the legal limit, it is not

significantly below. For this reason, the workstation, or any area that will be require

workers for any significant length of time will not be placed directly behind the outer

main shield. Finally, the dose rates at the top of the CONEX are presented in Figure

5.1.17.
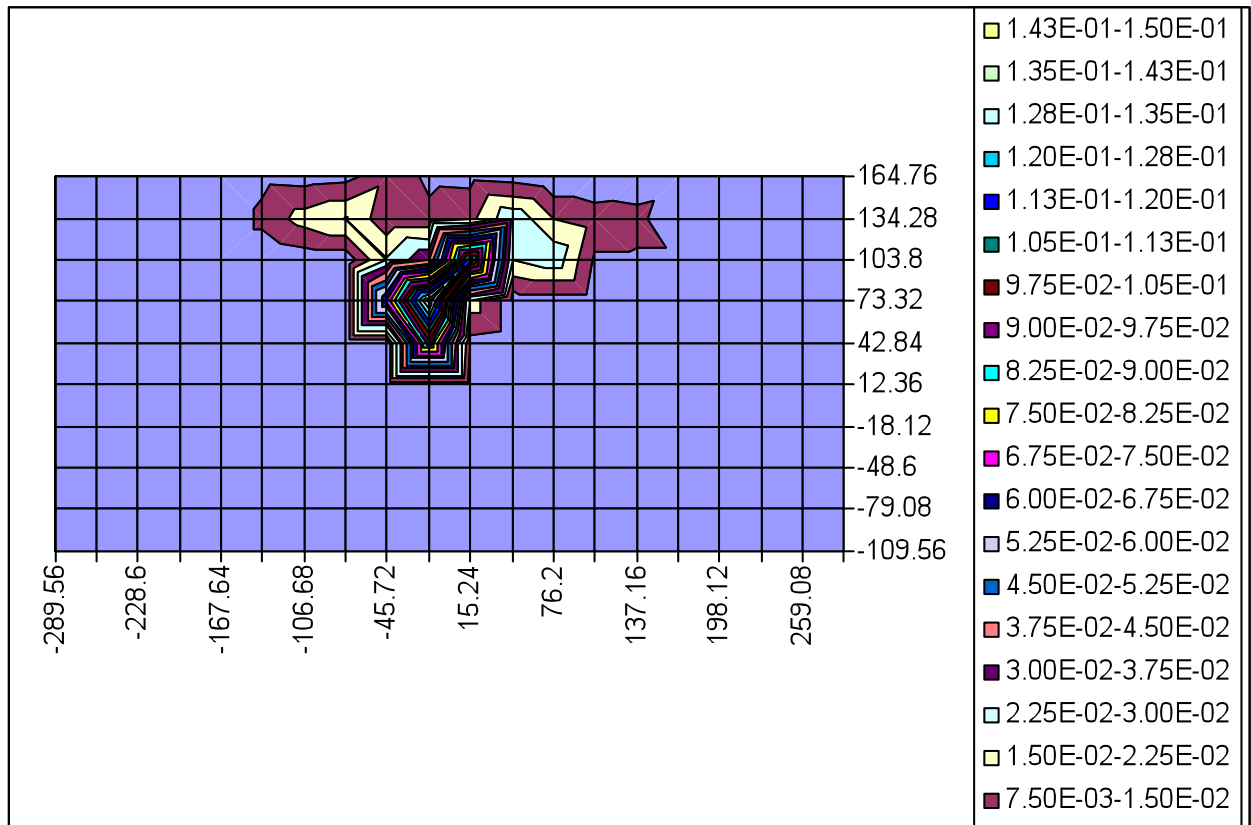
Figure 5.1.17: Dose rates on top of CONEX in REM/hr..

As can be seen from the above plot, the maximum dose rate delivered to the top

of the Conex is ~150 mRem/hr. Although this is 60 times higher than the targeted

2.5mRem/hr, there will be no access to the top of the Conex during operation. Even

should someone be exposed to the photon flux emanating from the top of the Conex, the

occupational limit would not be exceeded unless that person was exposed for over 33 hours.

Overall, the MCNP5 calculations show that with this shield design, workers can safely load the strawberries at a point 25' from the Conex and stay well below the occupation dose regulatory limits of 5 Rem/yr. This is due not only to the thickness of the shield, but also to the S-Shaped design that eliminates any source of unshielded streaming scattered photons that would suffer little geometric attenuation at this distance. Additional factors such as the low Z beam stop, minimized top shield, and the low proximity to the ground also minimize the dose rate outside of the shield while minimizing the mass required for the shield.

Weight Analysis:

As mentioned throughout, the weight of the shield was the primary issue. To minimize the shield weight while maintaining a level of economic viability, production rates were calculated as shown below in the food dose analysis. This ensures that the minimum flux necessary was used. Table 5.1.3 below shows the volume of material and Table 5.1.4 shows the weight for each shielding component.

Table 5.1.3: Volume of each shielding component in cm^3

	Outer Main Curvature	Inner Main Curvature	Main Top	Outer Secondary Curvature	Inner Secondary Curvature	Secondary Top
Lead	599,342	150,218	408,471	115,780	64,515	34,922
Poly	66,505	33,291	21,453	N/A	N/A	N/A
Aluminum	12,323	6,169	14,142	N/A	N/A	N/A
Steel	34,939	10,431	26,848	21,453	11,954	21,802

Table 5.1.4: Weight of each shielding component in lbs

	Outer Main Curvature	Inner Main Curvature	Main Top	Outer Secondary Curvature	Inner Secondary Curvature	Secondary Top
Lead	14,952	3,748	10,191	2,888	1,610	871
Poly	138	69	175	N/A	N/A	N/A
Aluminum	73	67	84	N/A	N/A	N/A
Steel	619	185	475	379	212	386

The total weight for the shield itself is 37,092 lbs, or 18.55 tons. This weight could further be reduced by a custom design that tapers off to a narrower thickness on the main outer curvature and top as the curve progresses further way from the beam source. This, however, is difficult to model in MCNP5 due to cell limitations on the number of characters used to describe the cells. As the number of cells increase, the method to

approximate this taper would require the shield to be segmented, the descriptions for the filling media, air in this instance, quickly surpasses the 1000 character limit resulting in a fatal error. Additionally, each run to further define the shield would require ~4 days to complete thereby required a long timetable with which to work with to completely refine the design and minimize weight.

Costs:

Costs for the shield will be primarily driven by material costs. Fabrication costs are estimated in the overall construction budget outlined in the cost analysis section of this report. Table 5.1.5 gives the approximate current price of various materials on a per unit and total basis[23,24].

Table 5.1.5: Estimated costs analysis for shielding materials based on current market prices[23,24]

	Lead	Polyethylene	Aluminum	Steel
Cost per lb	$0.60	$0.67	$0.68	$0.17
Total Cost	$20,556	$256	$131	$430

The total material cost for the shield is $21,373. This price will increase when one considers fabrication and design costs, but many of these costs are ties to the overall construction of the mobile e-beam irradiator and therefore are not estimated here. However, the material cost estimate shows that the shield costs is only a fraction of the overall system costs and not a limiting factor for economic feasibility of the entire system.

Future Areas for Improvement:

The shield design presented above, while carefully designed and maximized to reduce both the external dose and weight could be drastically improved with advanced modeling techniques. In particular, by segmenting the design into smaller portions, 30º sections as opposed the 180º sections modeled in Figure 5.1.6, the dose rate could be minimized by placing more shielding at the precise points needed while minimizing the weight by reducing the excess shielding at various points. Due to the fact that the outer main shield plus the top main shield constitutes ~65% of the overall shield weight but the vast majority of the external dose occurs only in a confined region, it is possible that the shield can be reduced to about 15 tons by this tapered approach to the shield thickness. Additional savings could be realized by custom building the secondary shields, but the savings from these regions wouldn't be nearly as large. Finally, savings could be realized in the reduction of the thickness in the top shield. Careful analysis of regulations and exposure effects from skyshine as well as scatter from the top of the conex would have to be studied to justify a higher dose rate than the one presented above, but a lot of weight could be saved should it be found safe and acceptable to lower the thickness of the top shield (The tapered approach above would certainly limit the thickness at carious points, but a reduction in the general thickness would realize large savings as well). This reduction in the weight of the shield would vastly improve the feasibility of such a device in the field.

Counteracting the obvious benefits to segmenting the shielding design is the intense computer simulation and modeling time needed. To accomplish the proposed design, it is possible that simplifications would have to be made regarding the

multilayered approach to shielding taken above. As was seen, this would dramatically affect the photon flux intensity and distribution primarily through the change in beam stop materials. These simplifications would be necessary due to the limitations in cell descriptions imposed by MCNP5 that would be strained as described above by the 6 fold increase in the number of cells.

Additional improvements could be made in the relative error of the dose rate estimates reported. In order to get the dose to below 2.5mRem/hr, the simulations only produced small numbers of photons which deposited energy in the outer tally volumes. Improvements in variance reduction coupled with longer run times would be necessary to produce improvements to acceptable levels.

5.2 Food Dose Analysis

Since strawberries are our primary food to be irradiated, a sample strawberry deck was created to be test the dose rates as a function of depth in the sample, determine raster rate, determine belt speed, determine necessary source power, and to determine the electron flux from the e-beam. First, the desired production rate had to be established.

Strawberries are hand picked by crews of 25-35 workers that can harvest and transport 4 flats containing 8 pts of strawberries each weighing ~1lb in an hour for a total hourly output per crew (35 workers) of ~500kg/hr[21]. Since this is the maximum rate that strawberries will be harvested at, it is desirable to design our system with this requirement in mind to minimize shielding.

Model:

The MCNP deck used to analyze the dose rate in strawberries is in included in Appendix I. The sample used was 1 window thick and three beam windows wide. The

source was moved along the sample to find the dose rates when the beam was centered, 1 beam window width off, two beam window widths off, and three beam widths off. This was then extrapolated into the matrix shown in Figure 5.2.1 below to calculate the total dose received in a cell per second. Cells beyond three off center were not included due to the insignificant overall contribution to the dose rate.

Figure 5.2.1: Matrix used to calculate the dose rate at each point of the strawberry

container

3 Off	3 Off	3 Off	3 Off	3 Off	3 Off	3 Off
3 Off	2 Off	2 Off	2 Off	2 Off	2 Off	3 Off
3 Off	2 Off	1 Off	1 Off	1 Off	2 Off	3 Off
3 Off	2 Off	1 Off	Centered	1 Off	2 Off	3 Off
3 Off	2 Off	1 Off	1 Off	1 Off	2 Off	3 Off
3 Off	2 Off	2 Off	2 Off	2 Off	2 Off	3 Off
3 Off	3 Off	3 Off	3 Off	3 Off	3 Off	3 Off

The beam width was calculated to have an angle of 13.5º. This is reflected in the SDEF card of the input deck in Appendix I. The plastic container that contained the strawberries was modeled as polyethylene. The container was assumed to contain 90% strawberries by volume. Strawberry composition, see Appendix II, was found and modeled[25] to accurately simulate the dose deposition throughout the volume. The container volume was divided into 0.25cm layers to analyze the dose rate as a function of

depth. Additionally, the conveyor was modeled to ensure contributions from backscatter and bremsstrahlung creation were accounted for.

Dose Deposition Results:

Table 5.2.1 shows the results obtained from the MCNP5 input deck. The results presented are simplified and the values obtained for 1, 2 and 3 off are taken as to be the same due to symmetry. This is not exactly true due to symmetry, but it will tend to overestimate the dose rate contribution from the elements on the corners which will be compensated for by the dose rate from when the beam is further than 4 window widths off. These contributions were then summed according to Figure 5.2.1 above for once and twice through (the product was flipped for the second run) and shown in Table 5.2.1 below.

Table 5.2.1: Dose Rates in Strawberries from 10 MeV electron beam with 1.1 cm^2

window

Depth (cm)	3 Off Dose (kGy/s)	2 Off Dose (kGy/s)	1 Off Dose (kGy/s)	Centered Dose (kGy/s)	Once Through Dose (kGy/s)	Twice Through Dose (kGy/s)
6.5	1.32E-02	5.41E-03	7.10E-03	8.07E-03	4.73E-01	3.39E+01
6.25	1.62E-02	4.80E-03	7.75E-03	9.83E-03	5.46E-01	3.88E+01
6	1.98E-02	5.34E-03	1.35E-02	1.81E-02	6.93E-01	4.26E+01
5.75	2.34E-02	8.61E-03	3.35E-02	5.10E-02	1.01E+00	4.52E+01
5.5	2.77E-02	2.28E-02	7.48E-02	1.13E-01	1.70E+00	4.70E+01
5.25	3.68E-02	5.31E-02	1.36E-01	2.07E-01	2.93E+00	4.87E+01
5	4.14E-02	1.00E-01	2.31E-01	3.24E-01	4.58E+00	4.98E+01
4.75	5.29E-02	1.55E-01	3.42E-01	4.74E-01	6.67E+00	5.07E+01
4.5	5.72E-02	2.21E-01	4.65E-01	6.57E-01	8.88E+00	5.07E+01
4.25	6.63E-02	3.01E-01	6.35E-01	8.83E-01	1.18E+01	5.04E+01
4	7.84E-02	3.81E-01	8.22E-01	1.16E+00	1.50E+01	4.99E+01
3.75	8.51E-02	4.63E-01	1.05E+00	1.51E+00	1.84E+01	4.91E+01
3.5	8.55E-02	5.55E-01	1.35E+00	1.96E+00	2.24E+01	4.91E+01
3.25	8.91E-02	6.35E-01	1.69E+00	2.52E+00	2.67E+01	4.91E+01
3	8.29E-02	6.84E-01	2.07E+00	3.20E+00	3.07E+01	4.91E+01
2.75	7.51E-02	7.24E-01	2.49E+00	4.05E+00	3.49E+01	4.99E+01
2.5	6.47E-02	6.99E-01	2.96E+00	5.07E+00	3.86E+01	5.04E+01
2.25	5.53E-02	6.26E-01	3.44E+00	6.31E+00	4.18E+01	5.07E+01
2	4.11E-02	5.08E-01	3.87E+00	7.78E+00	4.40E+01	5.07E+01
1.75	3.03E-02	3.67E-01	4.15E+00	9.49E+00	4.52E+01	4.98E+01
1.5	2.14E-02	2.28E-01	4.32E+00	1.14E+01	4.58E+01	4.87E+01
1.25	1.26E-02	1.25E-01	4.20E+00	1.35E+01	4.53E+01	4.70E+01
1	8.28E-03	6.46E-02	3.86E+00	1.59E+01	4.42E+01	4.52E+01
0.75	4.89E-03	3.50E-02	3.23E+00	1.86E+01	4.19E+01	4.26E+01
0.5	3.26E-03	2.28E-02	2.36E+00	2.13E+01	3.83E+01	3.88E+01
0.25	2.57E-03	1.22E-02	1.37E+00	2.35E+01	3.34E+01	3.39E+01

As can be seen in Table 5.2.1, the dose rates over the average time of irradiation accumulate to more than the 1 kGy limit for fruits and vegetables. This will be compensated for by rastering the beam across the 16" width of the strawberries. Additionally, the depth of penetration is small as seen in Figure 5.2.2; therefore, the product will be sent through twice. The dose rates for this twice through method are shown in Table 5.2.1 above.
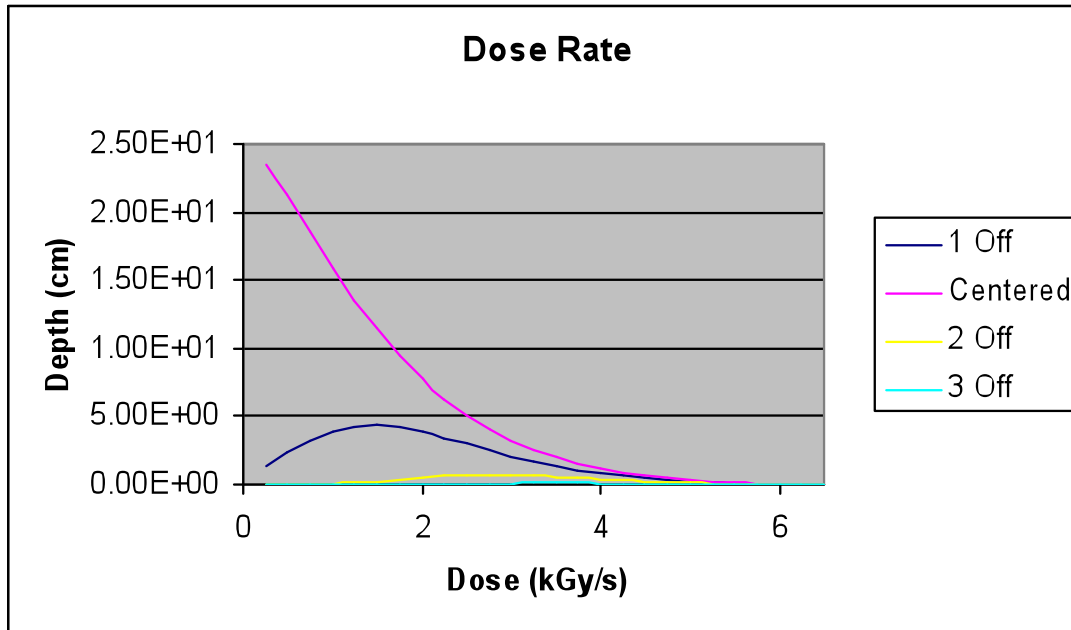
Figure 5.2.2: Dose rates as a function of depth for varying widow distances from the beam. The Curves represent the beam location with relation the volume where the dose rate is being tallies (i.e. 1 off means the beam window is 1 beam window distance away – 1.05cm).

To calculate the actual dose rate delivered throughout the product, the raster rate must be determined. The raster rate in Hz was found by the following formula:

Rate = $1/(1/D_{max})$

Where D_{max} = the maximum twice through rate in Figure 5.1.6 above (occurred at 2cm penetration)

The resulting raster rate is shown in Table 5.2.2 below along with the dose delivered at each depth. Figure 5.2.3 shows the depth-dose curve for strawberries based on this raster rate.
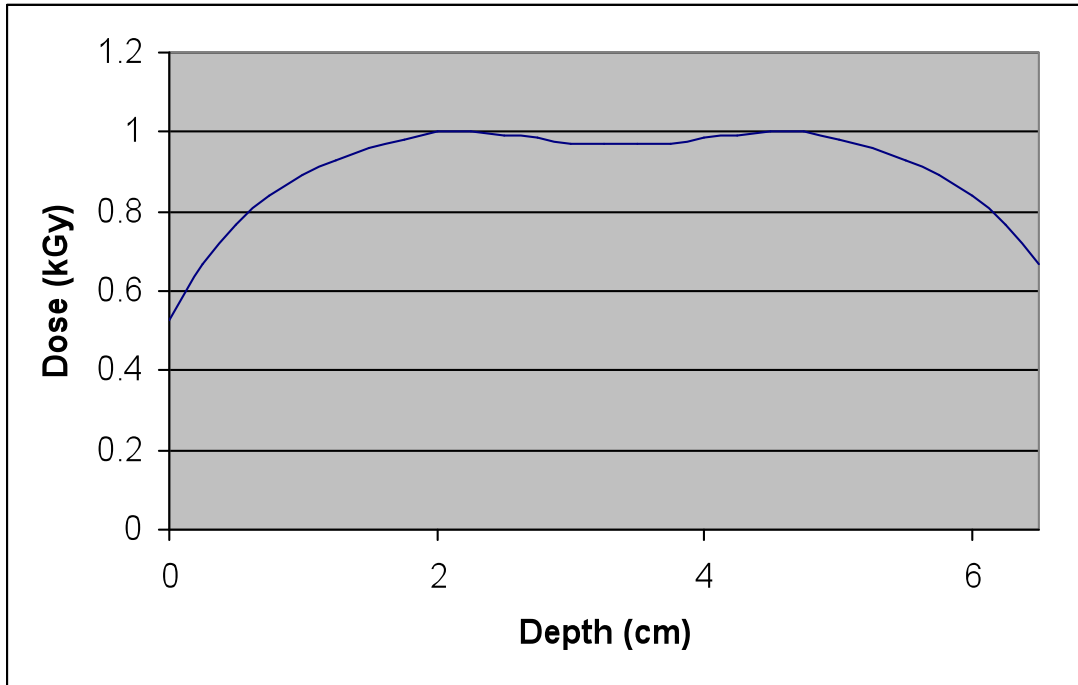
Figure 5.2.3: Dose as a function of depth for the twice through method accounting for

rastering rate

Table 5.2.2: Dose as a function of depth for a rastered beam

Dose for 50.7 Hz Raster Rate (kGy)	
0.25	6.68E-01
0.5	7.66E-01
0.75	8.40E-01
1	8.91E-01
1.25	9.26E-01
1.5	9.61E-01
1.75	9.81E-01
2	1.00E+00
2.25	1.00E+00
2.5	9.94E-01
2.75	9.84E-01
3	9.68E-01
3.25	9.69E-01
3.5	9.69E-01
3.75	9.68E-01
4	9.84E-01
4.25	9.94E-01
4.5	1.00E+00
4.75	1.00E+00
5	9.81E-01
5.25	9.61E-01
5.5	9.26E-01
5.75	8.91E-01
6	8.40E-01
6.25	7.66E-01
6.5	6.68E-01

As can be seen from Figure 5.1.7 and Table 5.1.6 above, a dose uniformity of ~ 66% is obtained by using this method. This is due to the peak of the off center dose rates near the 1/3 of the distance into the product as can be seen in Figure 5.1.7 above. The minimum dose of 0.668 kGy is plenty to extent shelf life and also kills a significant percentage of microbial pathogens as described in earlier sections.

Process Rates:

By obtaining the raster rate, the volumetric process rate and mass process rate can be determined. By determining the mass process rate, the beam power can be adjusted to

meet the desired production rate of ~500kg/hr calculated above. Table 5.2.3 below

shows the various values used to determine the mass process rate. Note that the mass

process rate allow for an additional 100kg/hr of processing capability to compensate for

non-continuous loading and/or higher output due to increased crew size or other factors.

Table 5.2.3: Mass Flow Calculations

Strawberry Density=	0.9225	**g/cm^3**
Volume of each cell=	0.275625	**cm^3**
Mass of each Cell =	0.254264063	**g**
Window Volume =	7.16625	**cm^3**
Beam Power=	200	**J/s**
10MeV beta=	1.60E-12	**J/e-**
Raster Rate	5.07E+01	**Hz**
Volume Process Rate =	3.63E+02	**cm^3/s**
Mass Process Rate =	3.35E-01	**kg/s**
Twice Through Process Rates		
Volume Process Rate =	6.54E+05	**cm^3/hr**
Mass Process Rate =	6.03E+02	**kg/hr**

To obtain belt speed for the strawberries, the size of the containers must be

defines. Typically strawberry containers are 4 15/16" x 7 7/16" x 3 1/2" in size. Due to

the limitation of 6.5 cm – 2 1/2" - in height, the strawberry container size for this process

is modified to 2.5" x 7.5" x 6.75". This provides a container of approximately the same

volume – 127 in^3 vs. 128 in^3 - while adhering to the restrictions on penetration imposed

by the e-beam. Typical flats contain 8 packages of strawberries making the flats used for

this process 2.5" x 15" x 27". Therefore, with the twice through method, 607.5' of

product will have to be processed per hour to obtain the mass process rates shown above.

For this, a forward belt speed of 10.125ft/min - 0.115 mph - will be needed.

These calculations show that a reasonable amount of strawberries, the maximum

amount typically picked on a large farm in an hr, can be processed by a beam with a

relatively low power setting as required by the shielding requirements.

Future Areas for Improvement:

These calculations can be improved upon by using better calculation tools and better defining the problem parameters. In particular, improvement in the strawberry model, primarily through better defining the density by volume of strawberry in a typical container, would improve the accuracy of the dose deposition rates. Additionally, a computer code that allowed for motion of the source and product would give more accurate dose deposition as a function of raster rate as compared to the stationary model proposed above that limited the range at which deposition was monitored.

6.0 Conclusions

Food irradiation is a safe process which can be utilized to prevent spoilage and increase the shelf-life of many foods. Several food irradiation facilities exist across the world at central locations. These facilities are generally large and intended for increasing shelf-lives and eliminating bacteria before shipping to distribution facilities. A problem with central facilities is that the food could experience spoilage before arrival at the facilities. A mobile food irradiation design could be useful in eliminating this problem by irradiating as soon as the foods are collected. This would require a much smaller design that would impose limits on shielding and as a result irradiation source. Therefore, the source chosen was an electron accelerator. These accelerators offer more safety features and require less shielding than would Co-60 or x-ray sources. However, an e-beam suffers from a lack of penetration. This would be compensated by irradiating small fruits or vegetables, particularly strawberries, in their smaller packages, as opposed to pallets.

These packages would also be flipped and run through the facility a second time to double the penetration. The design would consider safety, regulations, shielding requirements, components, and cost.

The electron beam produces 10 MeV pulses about 5 microseconds wide, with a frequency up to 300 pulses per second. The beam power is 1kW. The power requirement for the e-beam is 15kW 3 phase 208 volts. This will be provided by an external generator. A conveyor belt will be used to transport the food through the unit. The belt is stainless steel on the outside, and on the inside, the belt will be custom designed and made out of ultra-high molecular weight polyethylene which has been used before in x-ray machines.

The shielding has been designed, after several trials, to minimize the weight as well as dose to personnel. The conveyor was surrounded by shielding in an S-curve to minimize leakage of photons out of the conveyor inlet and outlet. The conveyor was also lowered to near the ground to utilize the ground as a primary shield. This allowed the design to remove the shielding on the bottom of the conveyor thus providing three sides of shielding. This helped in minimizing the weight of the shield. In order to minimize the amount of Bremsstrahlung produced, a low z material, polyethylene, was chosen as the first layer of shielding. The polyethylene would be surrounded by aluminum encasing. Lead was chosen as the second layer due to its high-density thus making the design more modular. The lead would be surrounded by steel to prevent exposure to lead. Steel would also be utilized as the material for the 20 ft X 8 ft X 8 ft Conex box.

A PLS truck was used to transport the design. The PLS is a military designed truck intended for extreme situations and heavy loads. It has the ability to place one container on its bed. The PLS can then unload this container onto the ground utilizing a

container handling unit. The design will utilize this in unloading the irradiator box to ground which is necessary for shielding requirements. A second container can be placed on a trailer behind the PLS. This container will house the external systems, such as the generator and control units.

Safety features were designed to ensure proper irradiation of the foods, proper placement on the ground, and safety of the workers. Dosimeters would be utilized in protecting the workers and ensuring the proper irradiation of the food. Records would be kept to ensure this and to follow regulations. An entry interlock and small openings at the conveyor inlet and outlet would prevent the workers from being exposed to irradiation. Ground sensors and an external generator would ensure that the unit is properly seated on the ground.

Using these design features, dose calculations were performed on the food and areas outside the Conex box housing the irradiator. These calculations were performed with MCNP5. Dose calculations showed that the majority of the dose is deposited in a region well inside the container. Although at the edge of the Conex box, the dose rates are slightly above the limits, at the administrative boundary 25 ft from the box, the dose rates are well below the established threshold. The calculations showed that workers could safely operate at the administrative boundaries, and still receive less than the dose regulatory limits of 5 Rem/yr.

Strawberry dose limits were then also calculated using MCNP. At 500 kg/hr, the facility would be capable of achieving the minimum and maximum dose limits of 0.4 and 1.0 kGy at a penetration of 6.5 cm.

These calculations show that this design would be capable of irradiating a reasonable amount of strawberries while providing the proper amount of shielding and safety.

This project was designed without the restrictions of a minimum or maximum cost considered. The total cost estimate which includes all of the major components required for a working mobile food irradiator, neglecting assembly and staff, is expected to be in the range of $1,346,464.

The approximate weight of main components for the mobile food irradiator will be at least 124,061 pounds. This weight is over the allowable 80,000 pound limit imposed in all 50 states, but permits can be acquired and escorts can be used to ensure safe travel to each destination.

7.0 Future Work

8.0 References

1. **Mount, John.** Science & Technology of Irradiation (Presentation). s.l. : Department of Food Science and Technology, University of Tennessee, 2009.

2. Pride of Hawaii. [Online] CW Hawaii Pride, LLC. http://www.hawaiipride.com/.

3. **Brennand, Charlotte P.** Food Irradiation. [Online] Idaho State University, March 1995. http://www.physics.isu.edu/radinf/food.htm.

5. FSIS Images. [Online] Food Safety and Inspection Service. http://www.fsis.usda.gov/News_&_Events/FSIS_Images/index.asp.

6. Van Tuyle, G. "Reducing RDD Concerns Related to Large Radiological Source Applications". LA-UR-03-6664. Los Alamos National Laboratory. Sept 2003.

7. Fan, Xuetong. "Finding a Kill Step - Is Irradiation the Answer". United Fresh Global FreshTech Conference April 26-28, 2007.

8. "Food Irradiation: A Safe Measure". U.S. Food and Drug Administration. Jan 2000.

9. Roberts, Tim. "Cold Pasteurization of Food By Irradiation ". Virigina Cooperative Education. Publication Number 458-300. Aug 1998.

10. **Turner, James.** *Atoms, Radiation and Radiation Protection.* 2nd. Weinheim : Wiley-VCH, 2004.

11. Title 21 - Food and Drugs. [Online] Food and Drug Administration, April 1, 2009. http://www.accessdata.fda.gov/scripts/cdrh/cfdocs/cfcfr/CFRSearch.cfm?CFRPart=179.

12. Federal Highway Administration, "Freight Management and Operations." US DOT 09 March, 2009. http://ops.fhwa.dot.gov/freight/size_weight.htm/

13. Oshkosh PLS Brochure. *Oshkosh Defense.* 2009.

14. **Sea Box, Inc.** 2009. 41235196d01.

15. US Land Warfare Systems. [Online] Federation of American Scientists. http://www.fas.org/man/dod-101/sys/land/.

16. **Dhaliwal, Amarjit S.** *Z-Dependence of Spectral Photon Energy Distributions of Thick Target Bremsstrahlung.* Department of Physics, Sant Longowal Institute of Engineering and Technology. s.l. : Longowal (Sangrur) 148106, Punjab, India, 2005. 148106.

17. **Weinhold, Bob.** Ozone Nation: EPA Standard Panned by the People. [Online] July 2008. http://www.pubmedcentral.nih.gov/articlerender.fcgi?tool=pmcentrez&artid=2453178.

18. **Health, National Institute for Occupational Safety and.** NTIS Publication No. PB-94-195047. [Online] May 1994. http://www.cdc.gov/niosh/idlh/intridl4.html.

19. **Air-Zone Air Purifiers.** Air-Zone - Ozone Meters and Ozone Sensors. [Online] April 20, 2009. http://www.air-zone.com/meter.html.

20. **Shultis, Kennith.** *Radiation Shielding.* Saddie River : Prentice Hall, 2000. 089448.

21. *Adjusting to Technological Change in Strawberry Harvest Work.* **Rosenberg, Howard R.** s.l. : Giannini Foundation of Agricultural Economics. http://www.agecon.ucdavis.edu/extension/update/articles/v7n1_2.pdf.

22. **Dorner Mfg. Corp.** Converor System. [Online] 2009. http://www.dornerconveyors.com/index.asp.

23. **IDES.** Street Plastic Prices Report. *The Plastics Web.* [Online] April 20, 2009. http://www.ides.com/resinprice/resinpricingreport.asp.
24. Current Primary and Scrap Metal Prices. [Online] April 20, 2009. http://www.metalprices.com/.

25. Ozcan, Mehmet Musa. *The Strawberry Fruits: Chemical Composition, Physical Properties and Mineral Contents.* University of Selcuk, Konya, Turkey . 2005.

Appendix I
Correspondence

James
Sorry I didn't get to you last week. Here's the answer to your e-mail if not
to your prayers.

These machines are built to a customer's requirements and are all specials.
We can tailor them to any special configuration.

The accelerator is typically four items, the beam head, the modulator/power
supply the TCU (cooler) and the control.

The beam head for the energy and power that you are looking for would be 60"
x 36" x 36". The electrons would exit one of the 36" square ends through the
scan horn which would project another 24". For an 18" scan width the horn would
be about 24" long by 4" wide. So the overall length would be 7 feet. If
necessary we could put in a bending magnet and the scan horn would attach to one of
the long sides near the end. It would be best to use the accelerator without
the bending magnet, you have the space to do this. The head would weigh 700
lb, without shielding.

The Modulator/power supply would be a rack 7' tall, 5' wide 4' deep. The
Modulator/power supply would weight 600 lb.

The TCU would be a refrigerated cooler 4' x 4' x 4'. This would need to have
access to the outside air to cool it. The TCU would weigh 500 lb.

The control would be a touch screen computer 24" x 18" x 5". This would weigh
50 lb.

In addition there would be cables, water pipes etc. which depending on length
could weigh another 500 lb.

The Modulator/power supply and control could sit in the second box.

We can supply 10 MeV and power 1 kW easily. The driver would be a magnetron.

The energy would be 10 MeV, the output 1 kW.

Power required is 15 kW 3 phase 208 volts 5 wire.

Approximate price $750,000 to $900,000 depending on final specification and
configuration.

The unit has a refrigerated cooler which can be placed outside.

The system would have complete safety systems, emergency switches on each
item. Tie in with external emergency switches. Most of the safety provisions
would be provided by the customer. We would be actively involved in advising this.
We can supply this if required. L&W refuses to sell equipment to a customer
who does not have adequate safety provisions, including shielding.

The electron beam would be 10 MeV pulses would be 5 microseconds wide, frequency up to 300 PPS.

You must address the shielding requirement. With this beam and energy the x-ray flux could be as much as 1000 R/min at a meter. You will need at least 1 foot of lead shielding. You will also need at least a double bend in the entry and exit passages to trap scattered radiation. You will also have to provide for X-rays scattering out of the ground if you use the ground as your primary shield.

That's enough to chew on, let me know how it goes.

Paul Leek

Appendix II

The following is MCNP5 code related to this project for strawberry dose deposition calculation.

```
10 MeV Beta Source Depositing into Strawberry Container
C Cell Cards
C Strawberry Cells (p=0.9225 g/cm^3 - 90% strawberry by volume)
1  100 -0.9225 -10 -40     imp:e=1 imp:p=1
2  100 -0.9225 -10 40 -41  imp:e=1 imp:p=1
3  100 -0.9225 -10 41      imp:e=1 imp:p=1
4  100 -0.9225 -11 -40     imp:e=1 imp:p=1
5  100 -0.9225 -11 40 -41  imp:e=1 imp:p=1
6  100 -0.9225 -11 41      imp:e=1 imp:p=1
7  100 -0.9225 -12 -40     imp:e=1 imp:p=1
8  100 -0.9225 -12 40 -41  imp:e=1 imp:p=1
9  100 -0.9225 -12 41      imp:e=1 imp:p=1
10 100 -0.9225 -13 -40     imp:e=1 imp:p=1
11 100 -0.9225 -13 40 -41  imp:e=1 imp:p=1
12 100 -0.9225 -13 41      imp:e=1 imp:p=1
13 100 -0.9225 -14 -40     imp:e=1 imp:p=1
14 100 -0.9225 -14 40 -41  imp:e=1 imp:p=1
15 100 -0.9225 -14 41      imp:e=1 imp:p=1
16 100 -0.9225 -15 -40     imp:e=1 imp:p=1
17 100 -0.9225 -15 40 -41  imp:e=1 imp:p=1
18 100 -0.9225 -15 41      imp:e=1 imp:p=1
19 100 -0.9225 -16 -40     imp:e=1 imp:p=1
20 100 -0.9225 -16 40 -41  imp:e=1 imp:p=1
21 100 -0.9225 -16 41      imp:e=1 imp:p=1
22 100 -0.9225 -17 -40     imp:e=1 imp:p=1
23 100 -0.9225 -17 40 -41  imp:e=1 imp:p=1
24 100 -0.9225 -17 41      imp:e=1 imp:p=1
25 100 -0.9225 -18 -40     imp:e=1 imp:p=1
26 100 -0.9225 -18 40 -41  imp:e=1 imp:p=1
27 100 -0.9225 -18 41      imp:e=1 imp:p=1
28 100 -0.9225 -19 -40     imp:e=1 imp:p=1
29 100 -0.9225 -19 40 -41  imp:e=1 imp:p=1
30 100 -0.9225 -19 41      imp:e=1 imp:p=1
31 100 -0.9225 -20 -40     imp:e=1 imp:p=1
32 100 -0.9225 -20 40 -41  imp:e=1 imp:p=1
33 100 -0.9225 -20 41      imp:e=1 imp:p=1
34 100 -0.9225 -21 -40     imp:e=1 imp:p=1
35 100 -0.9225 -21 40 -41  imp:e=1 imp:p=1
36 100 -0.9225 -21 41      imp:e=1 imp:p=1
37 100 -0.9225 -22 -40     imp:e=1 imp:p=1
38 100 -0.9225 -22 40 -41  imp:e=1 imp:p=1
39 100 -0.9225 -22 41      imp:e=1 imp:p=1
40 100 -0.9225 -23 -40     imp:e=1 imp:p=1
41 100 -0.9225 -23 40 -41  imp:e=1 imp:p=1
42 100 -0.9225 -23 41      imp:e=1 imp:p=1
43 100 -0.9225 -24 -40     imp:e=1 imp:p=1
44 100 -0.9225 -24 40 -41  imp:e=1 imp:p=1
45 100 -0.9225 -24 41      imp:e=1 imp:p=1
46 100 -0.9225 -25 -40     imp:e=1 imp:p=1
47 100 -0.9225 -25 40 -41  imp:e=1 imp:p=1
48 100 -0.9225 -25 41      imp:e=1 imp:p=1
49 100 -0.9225 -26 -40     imp:e=1 imp:p=1
50 100 -0.9225 -26 40 -41  imp:e=1 imp:p=1
51 100 -0.9225 -26 41      imp:e=1 imp:p=1
52 100 -0.9225 -27 -40     imp:e=1 imp:p=1
```

```
53 100 -0.9225 -27 40 -41  imp:e=1 imp:p=1
54 100 -0.9225 -27 41      imp:e=1 imp:p=1
55 100 -0.9225 -28 -40     imp:e=1 imp:p=1
56 100 -0.9225 -28 40 -41  imp:e=1 imp:p=1
57 100 -0.9225 -28 41      imp:e=1 imp:p=1
58 100 -0.9225 -29 -40     imp:e=1 imp:p=1
59 100 -0.9225 -29 40 -41  imp:e=1 imp:p=1
60 100 -0.9225 -29 41      imp:e=1 imp:p=1
61 100 -0.9225 -30 -40     imp:e=1 imp:p=1
62 100 -0.9225 -30 40 -41  imp:e=1 imp:p=1
63 100 -0.9225 -30 41      imp:e=1 imp:p=1
64 100 -0.9225 -31 -40     imp:e=1 imp:p=1
65 100 -0.9225 -31 40 -41  imp:e=1 imp:p=1
66 100 -0.9225 -31 41      imp:e=1 imp:p=1
67 100 -0.9225 -32 -40     imp:e=1 imp:p=1
68 100 -0.9225 -32 40 -41  imp:e=1 imp:p=1
69 100 -0.9225 -32 41      imp:e=1 imp:p=1
70 100 -0.9225 -33 -40     imp:e=1 imp:p=1
71 100 -0.9225 -33 40 -41  imp:e=1 imp:p=1
72 100 -0.9225 -33 41      imp:e=1 imp:p=1
73 100 -0.9225 -34 -40     imp:e=1 imp:p=1
74 100 -0.9225 -34 40 -41  imp:e=1 imp:p=1
75 100 -0.9225 -34 41      imp:e=1 imp:p=1
76 100 -0.9225 -35 -40     imp:e=1 imp:p=1
77 100 -0.9225 -35 40 -41  imp:e=1 imp:p=1
78 100 -0.9225 -35 41      imp:e=1 imp:p=1
C Define Plastic Container
85 300 -0.94   38 -39      imp:e=1 imp:p=1
C Conveyor Belt
86 400 -1.4   -50          imp:e=1 imp:p=1
87 400 -1.4   -51          imp:e=1 imp:p=1
C Define Air Fill
88 200 -0.0012 39 -60 #85 #86 #87  imp:e=1 imp:p=1
C Define Void
89    0     60          imp:e=0 imp:p=0


C Surface Cards
C Strawberry Layers
10  box 0   0   0.0 3.15 0 0  0 1.05 0  0 0 0.25  $ slice 1
11  box 0   0   0.25 3.15 0 0  0 1.05 0  0 0 0.25  $ slice 2
12  box 0   0   0.5 3.15 0 0  0 1.05 0  0 0 0.25  $ slice 3
13  box 0   0   0.75 3.15 0 0  0 1.05 0  0 0 0.25  $ slice 4
14  box 0   0   1.0 3.15 0 0  0 1.05 0  0 0 0.25  $ slice 5
15  box 0   0   1.25 3.15 0 0  0 1.05 0  0 0 0.25  $ slice 6
16  box 0   0   1.5 3.15 0 0  0 1.05 0  0 0 0.25  $ slice 7
17  box 0   0   1.75 3.15 0 0  0 1.05 0  0 0 0.25  $ slice 8
18  box 0   0   2.0 3.15 0 0  0 1.05 0  0 0 0.25  $ slice 9
19  box 0   0   2.25 3.15 0 0  0 1.05 0  0 0 0.25  $ slice 10
20  box 0   0   2.5 3.15 0 0  0 1.05 0  0 0 0.25  $ slice 11
21  box 0   0   2.75 3.15 0 0  0 1.05 0  0 0 0.25  $ slice 12
22  box 0   0   3.0 3.15 0 0  0 1.05 0  0 0 0.25  $ slice 13
23  box 0   0   3.25 3.15 0 0  0 1.05 0  0 0 0.25  $ slice 14
24  box 0   0   3.5 3.15 0 0  0 1.05 0  0 0 0.25  $ slice 15
25  box 0   0   3.75 3.15 0 0  0 1.05 0  0 0 0.25  $ slice 16
26  box 0   0   4.0 3.15 0 0  0 1.05 0  0 0 0.25  $ slice 17
27  box 0   0   4.25 3.15 0 0  0 1.05 0  0 0 0.25  $ slice 18
28  box 0   0   4.5 3.15 0 0  0 1.05 0  0 0 0.25  $ slice 19
29  box 0   0   4.75 3.15 0 0  0 1.05 0  0 0 0.25  $ slice 20
30  box 0   0   5.0 3.15 0 0  0 1.05 0  0 0 0.25  $ slice 21
31  box 0   0   5.25 3.15 0 0  0 1.05 0  0 0 0.25  $ slice 22
32  box 0   0   5.5 3.15 0 0  0 1.05 0  0 0 0.25  $ slice 23
33  box 0   0   5.75 3.15 0 0  0 1.05 0  0 0 0.25  $ slice 24
```

```
34  box 0    0   6.0  3.15 0 0  0 1.05 0  0 0 0.25  $ slice 25
35  box 0    0   6.25 3.15 0 0  0 1.05 0  0 0 0.25  $ slice 26
38  box 0    0   0   3.15 0 0  0 1.05 0  0 0 6.5  $ Encasing box
39  box -0.01 -0.01 -0.01 3.17 0 0  0 1.07 0  0 0 6.52  $ Encasing box
C Dividing Planes
40  px 1.05
41  px 2.10
C Conveyor Belt
50  box -5  -5  -0.01  13   0 0  0 13   0  0 0 -1.3
51  box -5  -5  -14.91 13   0 0  0 13   0  0 0 -1.3
60 s 2.1 0.5 3.5 25

C Data Cards
MODE E P
SDEF ERG=10.00 PAR=3 POS=1.575 0.525 9.06 VEC=0 0 -1 DIR=d3
sI3 -1 0 0.9725 1
sP3 0  0 0     1
PHYS:N J 20.
PHYS:P 10 0 0 0 0
PHYS:E 10 0 0 0 1
CUT:N 1.00
CUT:P 100.00000 0.001 0
CUT:E 100.00000 0.001  0
NPS 1000000
*F8:P,E   1
*F18:P,E  2
*F28:P,E  3
*F38:P,E  4
*F48:P,E  5
*F58:P,E  6
*F68:P,E  7
*F78:P,E  8
*F88:P,E  9
*F98:P,E  10
*F108:P,E 11
*F118:P,E 12
*F128:P,E 13
*F138:P,E 14
*F148:P,E 15
*F158:P,E 16
*F168:P,E 17
*F178:P,E 18
*F188:P,E 19
*F198:P,E 20
*F208:P,E 21
*F218:P,E 22
*F228:P,E 23
*F238:P,E 24
*F248:P,E 25
*F258:P,E 26
*F268:P,E 27
*F278:P,E 28
*F288:P,E 29
*F298:P,E 30
*F308:P,E 31
*F318:P,E 32
*F328:P,E 33
*F338:P,E 34
*F348:P,E 35
*F358:P,E 36
*F368:P,E 37
*F378:P,E 38
```

```
*F388:P,E 39
*F398:P,E 40
*F408:P,E 41
*F418:P,E 42
*F428:P,E 43
*F438:P,E 44
*F448:P,E 45
*F458:P,E 46
*F468:P,E 47
*F478:P,E 48
*F488:P,E 49
*F498:P,E 50
*F508:P,E 51
*F518:P,E 52
*F528:P,E 53
*F538:P,E 54
*F548:P,E 55
*F558:P,E 56
*F568:P,E 57
*F578:P,E 58
*F588:P,E 59
*F598:P,E 60
*F608:P,E 61
*F618:P,E 62
*F628:P,E 63
*F638:P,E 64
*F648:P,E 65
*F658:P,E 66
*F668:P,E 67
*F678:P,E 68
*F688:P,E 69
*F698:P,E 70
*F708:P,E 71
*F718:P,E 72
*F728:P,E 73
*F738:P,E 74
*F748:P,E 75
*F758:P,E 76
*F768:P,E 77
*F778:P,E 78
C Material Cards
m100 13000 0.02011  $Strawberry
     33000 0.01058
     5000  0.01603
     20000 4.95902
     48000 0.00019
     24000 0.00241
     29000 0.00165
     26000 0.01215
     31000 0.00047
     19000 14.90908
     3000  0.00094
     12000 1.31557
     25000 0.00444
     28000 0.00013
     15000 3.66856
     82000 0.00051
     38000 0.00510
     22000 0.00016
     23000 0.01663
     30000 0.00809
m200 7000  0.781    $Air
```

```
   8000  0.209
   18000 0.009
m300 1001  2        $Polyethylene
   6000  1
m400 6000  1         $Delrin
   1000  2
   8000  1
```

Appendix III

10 MeV Beta Source
C ****Changes: Add Poly on Bottom, 10cm Lead Top, Change AL to 0.25cm,
C **** Subtract 2cm poly from sides and top, 25cm lead outsides,2.5cm Conex
C **** New Conveyor Design, 20cm lead inside, 7cm lead curves
C Cell Cards
C Define Conveyor
1   600 -1.4   10 -11 -12 13 16 imp:e=1 imp:p=2
2   600 -1.4   10 -11 -14 15 16 imp:e=1 imp:p=2
3   800 -1.7 -10 17 -12 15 16 imp:e=1 imp:p=2
4   800 -1.7   11 -18 -12 15 16 imp:e=1 imp:p=2
5   600 -1.4   103 -104 -12 13 -16 imp:e=1 imp:p=2
6   600 -1.4   103 -104 -14 15 -16 imp:e=1 imp:p=2
7   800 -1.7 -103 101 -12 15 -16 imp:e=1 imp:p=2
8   800 -1.7   104 -102 -12 15 -16 imp:e=1 imp:p=2
9   600 -1.4   113 -114 -12 13 -16 imp:e=1 imp:p=2
101 600 -1.4   113 -114 -14 15 -16 imp:e=1 imp:p=2
102 800 -1.7 -113 111 -12 15 -16 imp:e=1 imp:p=2
103 800 -1.7   114 -112 -12 15 -16 imp:e=1 imp:p=2
C Define Conveyor Poly Shield
10 200 -0.94 -20 21 -24 25 27   imp:e=1 imp:p=16
11 200 -0.94   22 -23 -24 25 27   imp:e=1 imp:p=16
12 200 -0.94   20 -22 -24 26 27 28   imp:e=1 imp:p=16
13 200 -0.94   20 -22 25 -29 27   imp:e=1 imp:p=16
14 100 -2.7   -30 31 -34 35 37 #10 #12 #13   imp:e=1 imp:p=8
15 100 -2.7   32 -33 -34 35 37 #11 #12 #13   imp:e=1 imp:p=8
16 100 -2.7   30 -32 -34 36 37 38 #10 #11 #12 imp:e=1 imp:p=8
17 100 -2.7   30 -32 35 -39 37 #10 #11 #13   imp:e=1 imp:p=8
C Define Lead Shield
20 400 -8.05 -40   41 -44 45 47 #23 #25   imp:e=1 imp:p=32
21 400 -8.05   42 -43 -44 45 47 #24 #25   imp:e=1 imp:p=32
22 400 -8.05   40 -42 -44 46 47 38 #23 #24 #25 imp:e=1 imp:p=32
23 300 -11.34 -50   51 -54 55 57   imp:e=1 imp:p=32
24 300 -11.34 52 -53 -54 55 57   imp:e=1 imp:p=32
25 300 -11.34 50 -52 -54 56 57 28   imp:e=1 imp:p=32
26 400 -8.05 -121 122 -44 45 -47 #29 #121   imp:e=1 imp:p=32
27 400 -8.05   123 -124 -44 45 -47 #120 #121   imp:e=1 imp:p=32
28 400 -8.05   121 -123 -44 46 -47 #29 #120 #121 imp:e=1 imp:p=32
29 300 -11.34 -141 142 -54 55 -57   imp:e=1 imp:p=32
120 300 -11.34 143 -144 -54 55 -57   imp:e=1 imp:p=32
121 300 -11.34 141 -143 -54 56 -57   imp:e=1 imp:p=32
122 400 -8.05 -131 132 -44 45 -47 #125 #127   imp:e=1 imp:p=32
123 400 -8.05   133 -134 -44 45 -47 #126 #127   imp:e=1 imp:p=32
124 400 -8.05   131 -133 -44 46 -47 #125 #126 #127 imp:e=1 imp:p=32
125 300 -11.34 -151 152 -54 55 -57   imp:e=1 imp:p=32
126 300 -11.34 153 -154 -54 55 -57   imp:e=1 imp:p=32
127 300 -11.34 151 -153 -54 56 -57   imp:e=1 imp:p=32
C Define Conex
30 500 -0.0012 (-61:-64:-65:-66) #40 #1 #2 #3 #4 #5 #6 #7 #8 #9 #10
          #11 #12 #13 #14 #15 #16 #17 #20 #21 #22 #23 #24 #25 #26
          #27 #28 #29 #101 #102 #103 #120 #121 #122 #123 #124 #125
          #126 #127 imp:e=1 imp:p=4
31 400 -8.05 -62 imp:e=1 imp:p=32
C 32 300 -11.34 -61 62 imp:e=1 imp:p=32
33 400 -8.05 -60 61 64 65 66 imp:e=1 imp:p=8
C Define E-Beam
40 900 -2.0   -70   imp:e=1 imp:p=32
C Define Air in Shield
C 50 500 -0.0012 41 -43 -44 45 27 #1 #2 #3 #4 #5 #6 #7 #8 #9 #10 #11 #12
C   #13 #14 #15 #16 #17 #20 #21 #22 #23 #24 #25 #26 #27 #28

```
C          #29 #101 #102 #103  #120 #121 #122 #123 #124 #125 #126
C          #127 imp:e=1 imp:p=1
C Define Soil
80 700  -1.7   -81 60 imp:e=1 imp:p=1
C Define Water (Anthropomorphic Phantom Substitute)
90 1000 -0.0012 -91 60  #31 #80 imp:e=1 imp:p=32
C Define Void
91 0    91          imp:e=0 imp:p=0

C Surface Cards
C Curved Conveyor
10  CZ 64.2    $ Inner Radius of Curved End Belt
11  CZ 104.84  $ Outer Radius of Curved End Belt
12  PZ 25.78   $ Top of Top Belt (18" above ground)
13  PZ 24.48   $ Bottom of Top Belt (1.3cm thickness)
14  PZ 10.8    $ Top of Bottom Belt (14.9 cm conveyor thickness)
15  PZ 9.58    $ Bottom of Bottom Belt (1.3cm thickness)
16  PX 0       $ End of Curved Belt
17  CZ 60.68   $ Inside of Conveyor Sides
18  CZ 108.36  $ Outside of Conveyor Sides
C Poly-Shield - Conveyor
20  CZ 57.89   $ Inner Radius of Inner Poly Shield
21  CZ 54.89   $ Outer Radius of Inner Poly Shield
22  CZ 111.15  $ Inner Radius of Outer Poly Shield
23  CZ 114.15  $ Outer Radius of Outer Poly Shield
24  PZ 33.57   $ Top of Inner and Outer Poly Shield
25  PZ 2.25    $ Bottom of Inner and Outer Poly Shield
26  PZ 30.57   $ Bottom of Top Poly Shield
27  PX 0       $ End of Shield
28  C/Z 84.52 0 1.75 $ Beam Hole in Poly Shield
29  PZ 7.25    $ Top of Bottom Poly Shield
C Aluminum Casing For Poly - Conveyor
30  CZ 58.14   $ Inner Radius of Inner Al Casing
31  CZ 54.64   $ Outer Radius of Inner Al Casing
32  CZ 110.9   $ Inner Radius of Outer Al Casing
33  CZ 114.4   $ Outer Radius of Outer Al Casing
34  PZ 33.82   $ Top of Inner and Outer Al Casing
35  PZ 2.0     $ Bottom of Inner and Outer Al Casing
36  PZ 30.32   $ Bottom of Top Al Casing
37  PX 0       $ End of Shield
38  C/Z 84.52 0 1.5 $ Beam Hole in Poly Shield
39  PZ 7.5     $ Top of Bottom AL Casing
C Steel Casing for Lead - Conveyor
40  CZ 54.64   $ Inner Radius of Inner Steel Casing
41  CZ 34.64   $ Outer Radius of Inner Steel Casing
42  CZ 114.4   $ Inner Radius of Outer Steel Casing
43  CZ 139.4   $ Outer Radius of Outer Steel Casing
44  PZ 43.82   $ Top of Inner and Outer Steel Casing
45  PZ 2.0     $ Bottom of Inner and Outer Steel Casing
46  PZ 33.82   $ Bottom of Top Steel Casing
47  PX 0       $ End of Shield
C Lead Shield - Conveyor
50  CZ 54.14   $ Inner Radius of Inner Lead Shield
51  CZ 35.14   $ Outer Radius of Inner Lead Shield
52  CZ 114.9   $ Inner Radius of Outer Lead Shield
53  CZ 138.9   $ Outer Radius of Outer Lead Shield
54  PZ 43.32   $ Top of Inner and Outer Lead Shield
55  PZ 2.5     $ Bottom of Inner and Outer Lead Shield
56  PZ 34.32   $ Bottom of Top Lead Shield
57  PX 0       $ End of Shield
C Container
60  BOX -124.8 -304.8 2    304.8 0 0  0  609.6 0  0 0 213.36 $Outer CONEX
```

```
61  BOX  -122.3  -302.3  2      299.8 0 0  0  604.6 0  0 0 209.36 $Steel/Lead
62  BOX  -124.8  -304.8  0      304.8 0 0  0  609.6 0  0 0 2     $Outer CONEX Bottom
C 63  Box -149.8  -167.4  2      294.8 0 0  0  334.8 0  0 0 206.36 $Steel/Air
64  BOX  180  -229.72  9.58   -2.5 0 0  0 -47.68 0  0 0 24.25 $Conveyor Hole
65  BOX  180   229.72  9.58   -2.5 0 0  0  47.68 0  0 0 24.25 $Conveyor Hole
66  BOX  -10    -10    206.36 20   0 0  0  20   0  0 0 8    $Ventilation Hole
C E-Beam Machine
70  BOX  -76.2   -45.72  43.82 152.4 0 0  0  91.44 0  0 0 91.44
C Soil
81 box -1678.8  -1676.4 -30.48 3352.8 0 0  0 3352.8 0  0 0 30.48 $ Soil
C Tally Volume
91 box -1678.8  -1676.4 -30.48 3352.8 0 0  0 3352.8 0  0 0 500   $ Air
C Exit Curved Conveyor #1
101 C/Z 0 -169.04 60.68   $ Inside of Conveyor Sides
102 C/Z 0 -169.04 108.36  $ Outside of Conveyor Sides
103 C/Z 0 -169.04 64.2    $ Inner Radius of Curved End Belt
104 C/Z 0 -169.04 104.84  $ Outer Radius of Curved End Belt
105 PY  -169.04         $ End of Conveyor
C Exit Curved Conveyor #2
111 C/Z 0 169.04 60.68   $ Inside of Conveyor Sides
112 C/Z 0 169.04 108.36  $ Outside of Conveyor Sides
113 C/Z 0 169.04 64.2    $ Inner Radius of Curved End Belt
114 C/Z 0 169.04 104.84  $ Outer Radius of Curved End Belt
115 PY  169.04          $ End of Conveyor
C Exit Steel Casing #1
121 C/Z 0 -169.04 58.14   $ Inner Radius of Inner Steel Casing
122 C/Z 0 -169.04 51.14   $ Outer Radius of Inner Steel Casing
123 C/Z 0 -169.04 110.9   $ Inner Radius of Outer Steel Casing
124 C/Z 0 -169.04 117.9   $ Outer Radius of Outer Steel Casing
C Exit Steel Casing #2
131 C/Z 0 169.04 58.14   $ Inner Radius of Inner Steel Casing
132 C/Z 0 169.04 51.14   $ Outer Radius of Inner Steel Casing
133 C/Z 0 169.04 110.9   $ Inner Radius of Outer Steel Casing
134 C/Z 0 169.04 117.9   $ Outer Radius of Outer Steel Casing
C Exit Lead Shield #1
141 C/Z 0 -169.04 57.64   $ Inner Radius of Inner Lead Shield
142 C/Z 0 -169.04 51.64   $ Outer Radius of Inner Lead Shield
143 C/Z 0 -169.04 111.4   $ Inner Radius of Outer Lead Shield
144 C/Z 0 -169.04 117.4   $ Outer Radius of Outer Lead Shield
C Exit Lead Shield #2
151 C/Z 0 169.04 57.64   $ Inner Radius of Inner Lead Shield
152 C/Z 0 169.04 51.64   $ Outer Radius of Inner Lead Shield
153 C/Z 0 169.04 111.4   $ Inner Radius of Outer Lead Shield
154 C/Z 0 169.04 117.4   $ Outer Radius of Outer Lead Shield

C Data Cards
MODE E P
SDEF ERG=10.00 PAR=3 POS=84.52 0 30.32 VEC=0 0 -1 DIR=d3
sI3 -1 0 0.9725 1
sP3 0  0 0    1
BBREM 1 1 46i 100 100 200 300 400
PHYS:N J 20.
PHYS:P 10 0 0 0 0
PHYS:E 10 0 0 0 1
CUT:N 1.00
CUT:P 100.00000 0.001 0
CUT:E 100.00000 0.001  0
NPS 10000000
PRINT
C Tallies
FC14  Photon dose rate tally on top of Conex (1'x1'x7' volumes) - Shutlis AP
    - cSv/hr (rem/hr)
```

```
FMESH14:P  GEOM=xyz ORIGIN=-124.8 -304.8 213.36
      IMESH 180    IINTS 10
      JMESH 304.8  JINTS 20
      KMESH 396.24 KINTS 1
      out=ij
DE14 log 0.01 0.015 0.02 0.03 0.04 0.05 0.06 0.08 0.1 0.15 0.20 0.30 0.4 0.5 0.6
   0.8 1.0 2.0 4.0 6.0 8.0 10
DF14 log 0.0496E-12 0.129E-12 0.211E-12 0.307E-12 0.345E-12 0.363E-12
   0.382E-12 0.441E-12 0.519E-12 0.754E-12 1.00E-12 1.51E-12 2.00E-12
   2.47E-12 2.91E-12 3.73E-12 4.48E-12 7.45E-12 11.9E-12 15.7E-12
   19.3E-12 23.0E-12
FM14  4.49E19
FC24  Photon dose rate tally (1'x1'x7' volumes) - Shultis AP
   - cSv/hr (rem/hr)
FMESH24:P  GEOM=xyz ORIGIN=-886.8 -1066.8 0.00
      IMESH 942    IINTS 60
      JMESH 1066.8 JINTS 70
      KMESH 213.36 KINTS 1
      out=ij
DE24 log 0.01 0.015 0.02 0.03 0.04 0.05 0.06 0.08 0.1 0.15 0.20 0.30 0.4 0.5 0.6
   0.8 1.0 2.0 4.0 6.0 8.0 10
DF24 log 0.0496E-12 0.129E-12 0.211E-12 0.307E-12 0.345E-12 0.363E-12
   0.382E-12 0.441E-12 0.519E-12 0.754E-12 1.00E-12 1.51E-12 2.00E-12
   2.47E-12 2.91E-12 3.73E-12 4.48E-12 7.45E-12 11.9E-12 15.7E-12
   19.3E-12 23.0E-12
FM24  4.49E19
FC34  Photon dose rate tally in Conex (1'x1'x7' volumes) - Shutlis AP
   - cSv/hr (rem/hr)
FMESH34:P  GEOM=xyz ORIGIN=-124.8 -304.8 0.00
      IMESH 180    IINTS 10
      JMESH 304.8  JINTS 20
      KMESH 213.36 KINTS 1
      out=ij
DE34 log 0.01 0.015 0.02 0.03 0.04 0.05 0.06 0.08 0.1 0.15 0.20 0.30 0.4 0.5 0.6
   0.8 1.0 2.0 4.0 6.0 8.0 10
DF34 log 0.0496E-12 0.129E-12 0.211E-12 0.307E-12 0.345E-12 0.363E-12
   0.382E-12 0.441E-12 0.519E-12 0.754E-12 1.00E-12 1.51E-12 2.00E-12
   2.47E-12 2.91E-12 3.73E-12 4.48E-12 7.45E-12 11.9E-12 15.7E-12
   19.3E-12 23.0E-12
FM34  4.49E19
C Material Cards
m100 13000 1          $Aluminum
m200 1001  2          $Polyethylene
   6000  1
m300 82204 0.014      $Lead
   82206 0.241
   82207 0.221
   82208 0.524
m400 6000  -0.05      $Steel 1050
   15000 -0.05
   19000 -0.04
   25000 -0.90
   26000 -98.96
m500 6000  -0.000127  $Air
   7000  -0.76508
   8000  -0.234793
m600 6000  1          $Delrin
   1000  2
   8000  1
m700 8000  -0.467     $Soil
   14000 -0.27
   13000 -0.081
```

```
     26000 -0.05
     11000 -0.02
     12000 -0.02
     19000 -0.02
     20000 -0.02
     15000 -0.026
     16000 -0.026
m800 1000  2          $Conveyor Sides
     6000  1
     8000  1
     13000 0.25
m900 13000 -0.70      $E-Beam
     7000  -0.23
     8000  -0.07
m1000 1000 2          $Water
     8000 1
```